International Journal of Earth Sciences
https://doi.org/10.1007/s00531-021-02138-1

ORIGINAL PAPER

REE mineralization related to carbonatites and alkaline magmatism in the northern Tarim basin, NW China: implications for a possible Permian large igneous province

Mingcai Xie[1,2] · Wenjiao Xiao[1,2,3] · Benxun Su[1,2] · Patrick Asamoah Sakyi[4] · Songjian Ao[1] · Jien Zhang[1] · Dongfang Song[1] · Zhiyong Zhang[1] · Zhiyuan Li[1,2] · Chunming Han[1,2,3]

Received: 14 July 2021 / Accepted: 15 November 2021

Abstract
Permian magmatism occurred widely in the Tarim basin and adjacent areas of NW China, resulting in the emplacement of numerous carbonatite plutons and alkaline rock intrusions, which are likely to have been derived from mantle sources. In addition, at least one large igneous province (LIP) can be recognized in NW China; namely, the ca. 270–290 Ma Tarim LIP, and it can be inferred that the peak age of magma activity is ~ 280 Ma. Therefore, the mantle plume is limited spatially within southern Tianshan and the Tarim Basin and temporally in the Early Permian. Age and field evidence suggest a spatial and temporal relationship between the carbonatites and alkaline rocks within the Tarim LIP, and their genesis is related to the Tarim mantle plume. In this paper, we direct our attention to the mineral assemblages that are related to carbonatites and alkaline rocks which host REE deposits (Wajilitag, Boziguoer) in the northern Tarim Craton. Alkaline rocks typically are related to rifts and/or extensional tectonics, and we suggest that these magmatic and metallogenic events occurred during an extensional regime, possibly related to the Tarim mantle plume event that affected much of South Tianshan during the Permian.

Keywords Tarim · Carbonatite and alkaline · Large igneous provinces · Mantle plume

Introduction

Large igneous provinces (LIPs) are not only an important window into geological processes and biospheric extinctions in the deep earth, but they are often accompanied by the formation of numerous deposit types of important economic value, leading to the extreme enrichment of important strategic resources (Begg et al. 2010; Jowitt et al. 2014). In the formation process of LIPs, a large amount of basaltic magma is generated in a short time, which create favorable metallogenic conditions for large-scale chromite deposits, copper-nickel sulfide deposits, Fe–Ti oxide deposits and other magmatic deposits (Hu et al. 2005; Song et al. 2010). Many superlarge magmatic deposits form in LIPs, a typical representative of which is the Noril'sk-Talnakh superlarge Ni–Cu-PGE sulfide deposits of the Siberian LIP (Naldrett 1992; Arndt et al. 2003), the Skaergaard Pd–Au deposits in North Atlantic LIP (Andersen et al. 1998; Holwell and Keays 2014), the Panxi Fe–Ti–V deposits in the Emeishan LIP (Zhang et al. 2009a, b; Song et al. 2013) and the Brandberg REE deposits in the Paraná-Etendeka LIP (Ernst and Buchan 2001).

Widespread Permian carbonatite-alkaline rocks have been discovered in the Tarim Basin and adjacent areas (Xu et al. 1998; Zou et al. 1998, 2002; Liu et al. 2004; Li and Yan 2015). These carbonatite-alkaline rocks start from Tuoyun of Atushi in the west and extend to the east of Yuli County in the east (Fig. 1b; Zou et al. 2002). In the alkaline rock belt on the Tarim Basin's northern margin, some REE deposits

✉ Chunming Han
cm-han@mail.iggcas.ac.cn

1 Key Laboratory of Mineral Resource, Institute of Geology and Geophysics, Chinese Academy of Sciences, Beijing 100029, China

2 College of Earth and Planetary Sciences, University of Chinese Academy of Sciences, Beijing 100049, China

3 CAS Center for Excellence in Tibetan Plateau Earth Sciences, Beijing 100101, China

4 Department of Earth Science, School of Physical and Mathematical Sciences, University of Ghana, P.O. Box LG 58, Legon-Accra, Ghana

Published online: 30 November 2021

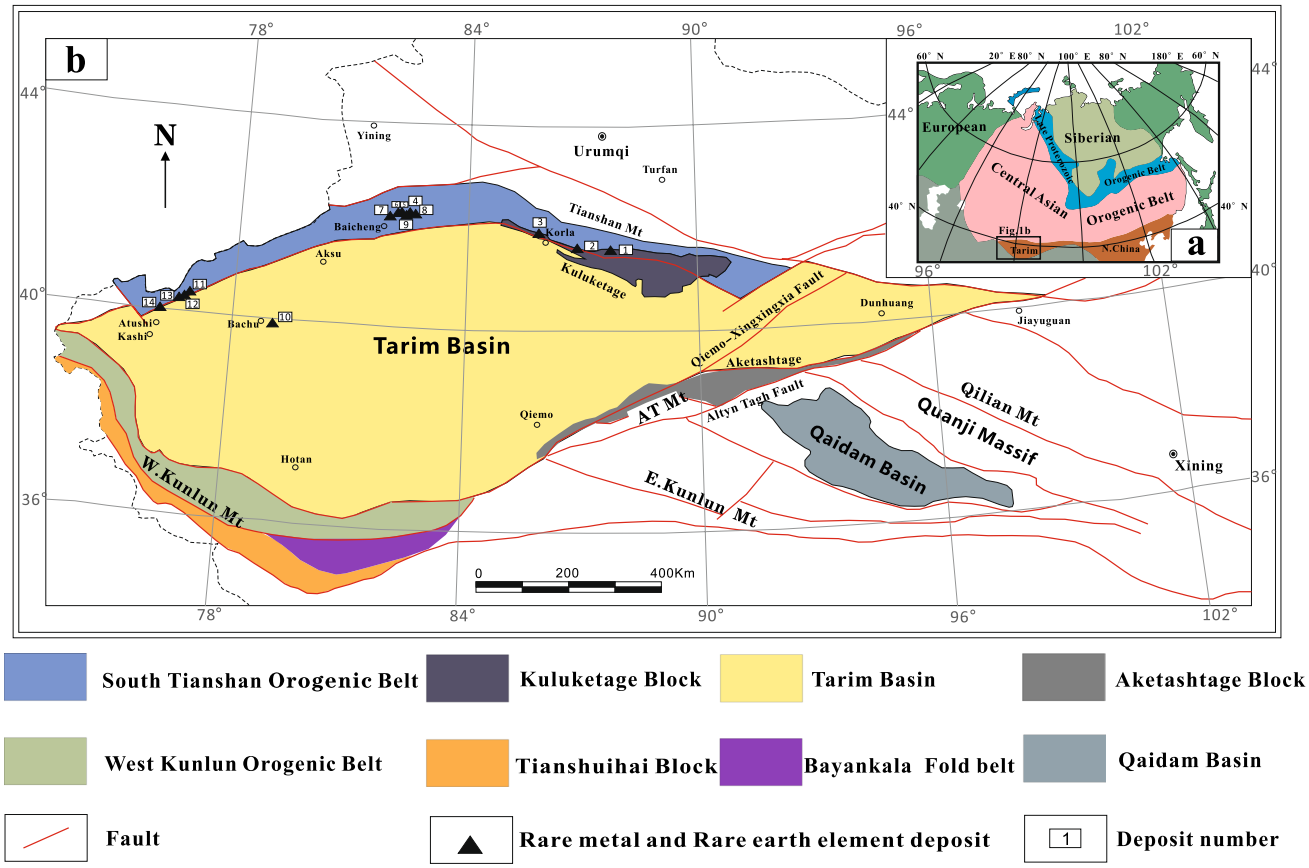

Fig. 1 **a** Tectonic sketch map of the Central Asian Orogenic Belt showing the position of the alkaline rock belt (modified from Gao et al. 2011; Huang et al. 2014). **b** Tarim Craton and its surrounding geotectonic map related to rare metal-rare earth element deposits (modified from Lu et al. 2008)

(ore occurrences) with economic prospects have been discovered (Table 1), to have primarily formed in the Permian. In spite of the numerous studies (e.g., Xu et al. 1999; Zou et al. 2002; Liu et al. 2004; Yin et al. 2013; Li and Yan 2015) that have been carried out, the origin of the Permian carbonatite-alkaline intrusions in the Tarim Basin is poorly understood, and the nature of their mantle sources is still unknown. Many geologists have conducted many studies on these carbonatite-alkaline rocks and associated REE deposits (Zou et al. 2002; Zou and Li 2006; Liu et al. 2012, 2013; Xu et al. 2010, 2012; Huang et al. 2014, 2018). However, there have not been extensive reviews in the English language relating the tectonic evolution of the Tarim LIP to the different types of REE deposits in the north of the Tarim LIP. As a result, the international geological community knows little about this tectonic relationship. In this contribution, we present a detailed overview of the geological characteristics of typical REE deposits related to the carbonatite-alkaline rocks in the northern margin of the Tarim Basin, with emphasis on their mineralization, metallogenetic timing and associated lithologies, which will provide insights into the tectonic evolution of the Tarim LIP.

Geological setting

The South China, North China and Tarim Cratons make up the tectonic framework of China (Zhao and Cawood 2012). The Tarim Craton has a late Archean to Paleoproterozoic basement similar in lithology and age to that of the Western Block of the North China Craton, and has no clear suture zone with the latter (Zhao et al. 2001). The Tarim Craton is bounded by the Tianshan, Western Kunlun and Central-Southern Altyn Tagh mountain belts to the north, south and southeast, respectively (Fig. 1b; Lu et al. 2008; Zhang et al. 2013b). More than 85% of the Tarim Craton is covered by desert with Precambrian basement rocks only exposed on the margins of the craton, including the Hetian area in the southwestern margin, the Akesu area in the northwestern margin, the Kuluketage area in the northeastern margin, the North Altyn Tagh Mountain and the Dunhuang area in the eastern margin. Due to its inadequate exposure, the Tarim Craton has not been comprehensively studied, but in the last few years Chinese researchers have carried out extensive field-based

Table 1 Characteristics of rare-rare earth deposits associated with alkaline rocks in the northern margin of Tarim Craton

Ore deposits (occurrence)	Location	Long./lat	Type	Ore minerals	Host rocks	Main economic elements	Grade	Age, Ma	References
Kuoktag (1)	Yuli County	88°26′09″ 41°05′13″	Alkaline syenite type	Pyrochlore, Zircon, Allanite, Columbite, Titanite, Chevkinite	Pt Xingditage Group marble and schist	Nb, Ta, Zr, REE	RE_2O_3:0.0984%; Nb_2O_5:0.0544%; Ta_2O_5:0.0068%; (Zr,Hf)O_2:0.1058%~0.4613	Aegirine albite: Rb–Sr: 249; zircon U–Pb: 224±2	Zou et al. 2002, 2006); Wang 2003); Guo et al. (2013)
Qieganbulak (2)	Yuli County	87°34′00″ 41°12′56″	Carbonatite type	Apatite	Pt Xingditage Group marble and schist	REE, P	RE_2O_3: 0.087%~0.163, P_2O_5: 1%~8%①	Whole rock Sm–Nd: 802±52; Phlogopite $^{39}Ar/^{40}Ar$: 811.9±1.1; Pyroxenite zircon U–Pb:811±12	Yin 1992); Jiang et al. (2005); Sun et al. 2007); Huang et al. 2012a, b); Ye (2014)
Shanghu (3)	Korla	86°00′16″ 41°52′20″	Pegmatite type	Allanite, Ilmenite, Zircon, Limonite, Pyrite	Pt Xingditage Group migmatite, marble and schist	REE	Orebody RE1, RE_2O_3: 1.01%~5.1%; OrebodyRE2, RE_2O_3: 1.62%~1.84%; OrebodyRE3, RE_2O_3: 2.64%~3.93%	Zircon U–Pb: 1810	Zhang (2019)
Yilanlik (4)	Baicheng County	82°36′45″ 42°29′42″	Alkaline pegmatite type	Monazite, Zircon, Thorite, Uraninite, Diopside, Sodalite, Samarskite	O-S Marble, skarn, hornstone, schist	REE, Nb, Ta, Zr	RE_2O_3: 1.559%; Ta_2O_5: 0.070%; Nb_2O_5: 0.022%; ZrO_2:0.040%	Biotite granite, zircon U–Pb: 269	Zou et al. (2006); Xu et al. 1998); Zou et al. (2002)
Keqikeguole (5)	Baicheng County	82°09′00″ 42°19′30″	Alkaline syenite type	Zircon, Columbite	S_3 Aegirine-Augite albitite at the top of alkaline stock	Nb, Zr	Nb_2O_5:0.0231%~0.0364; ZrO_2: 0.1668%~0.2773%	Neirine syenite, zircon: 279	Zou et al. (2006); Xu et al. 1998); Zou et al. 2002
Tasiduwei (6)	Baicheng County	82°09′24″ 42°19′08″	Carbonatite type	Apatite	S_3 Carbonated lava	REE	RE_2O_3:0.037%~0.111%	—	Zou et al. (2002)
Boziguoer (7)	Baicheng County	81°54′30″ 42°13′30″	Alkaline granite type	Pyrochlore, Xenotime, Zircon, Thorite, Monazite, Columbite	S_3 Keketiekedaban Formation marble	REE, Nb, Ta, Zr	RE_2O_3: 0.07%~0.19%; Y_2O_3: 0.04%~0.06%; Nb_2O_5: 0.1987%; Ta_2O_5: 0.0211%; (Zr,Hf)O_2: 0.15%~1.68%	Biotite potassium feldspar granite, zircon: 275±1.4; Aegirine albite granite, zircon: 290.1±1.4	Zou et al. 2002); Xu et al. 2010, 2012); Huang et al. (2014)

Table 1 (continued)

Ore deposits (occurrence)	Location	Long./lat	Type	Ore minerals	Host rocks	Main economic elements	Grade	Age, Ma	References
Mayida (8)	Baicheng County	82°39′52″ 42°28′20″	Alkaline pegmatite type	Monazite, Zircon, Columbite, Thorite, Sodalite	Pt_3 Marble and hornstone; S_{1-2} Scapolite marble interlaced with granulite and schist	REE, Nb, Ta, Zr	RE_2O_3:0.013%~0.292%; Y_2O_5: 0.005%~0.053%; Nb_2O_5: 0.005%~0.598; Ta_2O_5: 0.002%~0.026%: ZrO_2: 0.008%~0.353	—	Zou et al. (2002)
Kajiwusi (9)	Baicheng County	82°37′56″ 42°29′12″	Alkaline pegmatite type	Diopside, Sodalite	Pt_3 Marble and hornstone; S_{1-2} Scapolite marble interlaced with granulite and schist	Nb, Ta, Zr, REE	Gem grade diopside: 0.5 kg/m^3~1 kg/m^3	—	Zou et al. (2002)
Wajilitag (10)	Bachu County	78°53′45″ 39°34′52″	Carbonatite type	Monazite, Bastnaesite, Pyrochlore, Apatite	$D_{1-2}y$, Yimugantawu Formation; D_3k, Keziletage Formation	REE, Nb, P	RE_2O_3: 1.43%~5.91%; P_2O_2: 0.99%~16%; Nb_2O_3: 0.005%~0.29%	Nepheline syenite & carbonatite:273	Li (2001); Zou et al. (2002); Jiang et al. 2004a, b, c); Li et al. 2015); Jin et al. (2019)
Huoshibulake (11)	Atushi	77°21′46″ 40°31′55″	Alkaline granite type	Zircon, Apatite, Fluorite, Tourmaline	P, Sedimentary rocks	REE	RE_2O_3:2.433%	Alkali feldspar granite, zircon U–Pb: 278±3	Zou et al. 2002); Zhang et al. (2010a, b, (c)
Tamu (12)	Atushi	77°12′07″ 40°22′22″	Alkaline granite type	Zircon, Columbite, Apatite	P, Sedimentary rocks	Nb, Zr	Nb_2O_5: 0.0173%; Columbite: > 70 g/t; Zircon: ~300 g/t	—	Zou et al. 2002); Huang et al. 2012a, (b)
Tamuxi (13)	Atushi	77°08′31″ 40°20′22″	Hydrothermal quartz vein type	Gem	P, Sedimentary rocks	—	—	Alkaline granite:275	Zou et al. (2002); Xu et al. (2012)
Bashisuogong (14)	Atushi	76°30′00″ 40°03′00″	Alkaline granite type	Columbite, Pyrochlore, Fergusonite	P_1b, Balikelik Formation clastic rocks and carbonate rocks	Nb, Ta, REE	Nb_2O_5: 0.018%	Gabbro, zircon U–Pb: 273.95±0.85; Quartz syenite, zircon U–Pb: 268.9±1.0	Yang et al. ((2016)

① According to the Geological Survey Institute of Xinjiang Uygur Autonomous Region

structural, petrological, geochemical and geochronological investigations on the basement of the craton (Xu et al. 2005; Lu et al. 2008; Long et al. 2010, 2011a, 2012; b; Shu et al. 2011; Zhang et al. 2013b).

The Tarim LIP consists of tholeiitic volcanic rocks, mafic dykes, mafic–ultramafic rocks and syenites covering an area of about 250,000 km^2 and with a thickness of between 600 and 800 m, in the western and southwestern parts of the Tarim Basin (Fig. 2; Jia et al. 1995; Jiang et al. 2004c, 2006; Xia et al. 2004; Yang et al. 2006a, b, c; Zhang et al. 2008). The timing of the Tarim LIP igneous suites is between 290 and 275 Ma (Li et al. 2008, 2011; Chen et al. 2009), with the large-scale basaltic magma eruption that occurred between ca. 290 and 288 Ma (Yu et al. 2011). The basalts from the Keping area have an OIB-like (OIB: oceanic island basalt) trace element pattern with enrichments in LILEs (large ion lithophile elements) and HFSEs (high field strength elements), a relatively high $^{87}Sr/^{86}Sr_i$ and negative $\varepsilon_{Nd}t$) value suggesting that they were derived from an enriched mantle (Zhou et al. 2009; Zhang et al. 2010b). The basalts should reflect an interaction between the mantle plume and the lithosphere (Yu et al. 2009, 2011; Zhang et al. 2010c; Wei and Xu 2013; Wei et al. 2014a). The generation of the intermediate-felsic volcanic rocks in the northern Tarim Block, Bachu syenites (A-type granite) and syenitic porphyry and the Halajun A-type granite correlate with the mantle plume and the appearances of A-type granite means the end of the Tarim LIP magmatism (Chen et al. 1998; Yang et al. 2006a, b; Sun et al. 2007; Zhang et al. 2010a, b). All the geological characteristics, such as the large-scale crustal uplift (Chen et al. 2006; Li et al. 2014), the identical geochemical features displayed by the ultrabasic rocks and the picrite (Yang et al. 2007a, b; Tian et al. 2010), and the large scale of dyke swarms and V–Ti magnetite deposit support the theory that the Tarim LIP is related to mantle plume magmatism. Permian intrusions in the Tarim Basin and surrounding areas include carbonatites and alkaline plutons (Yang et al. 2006a, b; Zhang et al. 2008, 2010a, b). The carbonatites in the Bachu area intruded into the layered mafic–ultramafic intrusions in Devonian strata and are subsequently cut by diabase dykes (Fig. 3; Cheng et al. 2018). The alkaline rocks are approximately east–west trending, which runs from Atushi in the west, through Bachu, Aksu, Baicheng and Korla in the east, to the east of Yuli County, and reaches the Tarim Fault Zone in the south, with a length of 1100 km. One of the largest manifestations of alkaline ultramafic magmatism with carbonatites is the Bachu area that includes the Wajilitag complex as well as a number of other complexes occurring mainly within the South Tianshan along the northern margin of Tarim Craton (Zou and Li 2006).

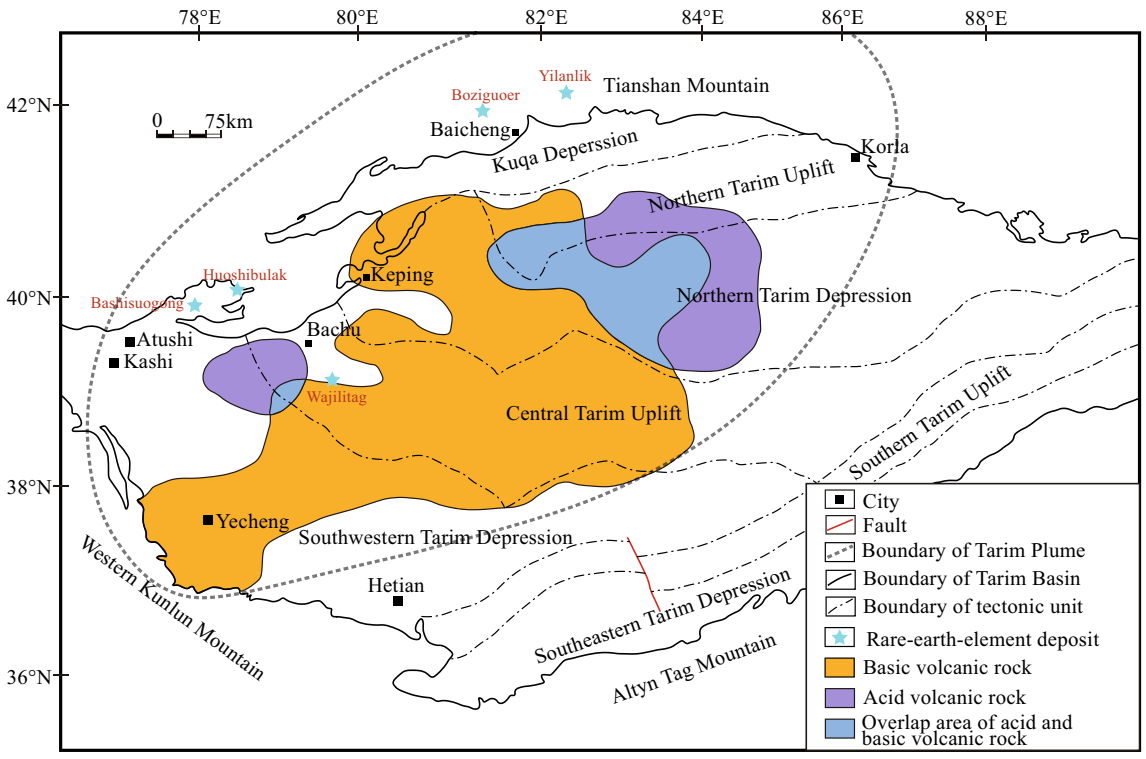

Fig. 2 The distribution of the Tarim Large Igneous Province, showing the locations of important REE deposits related to carbonatites and alkaline magmatism (modified from Yang et al. 2007b)

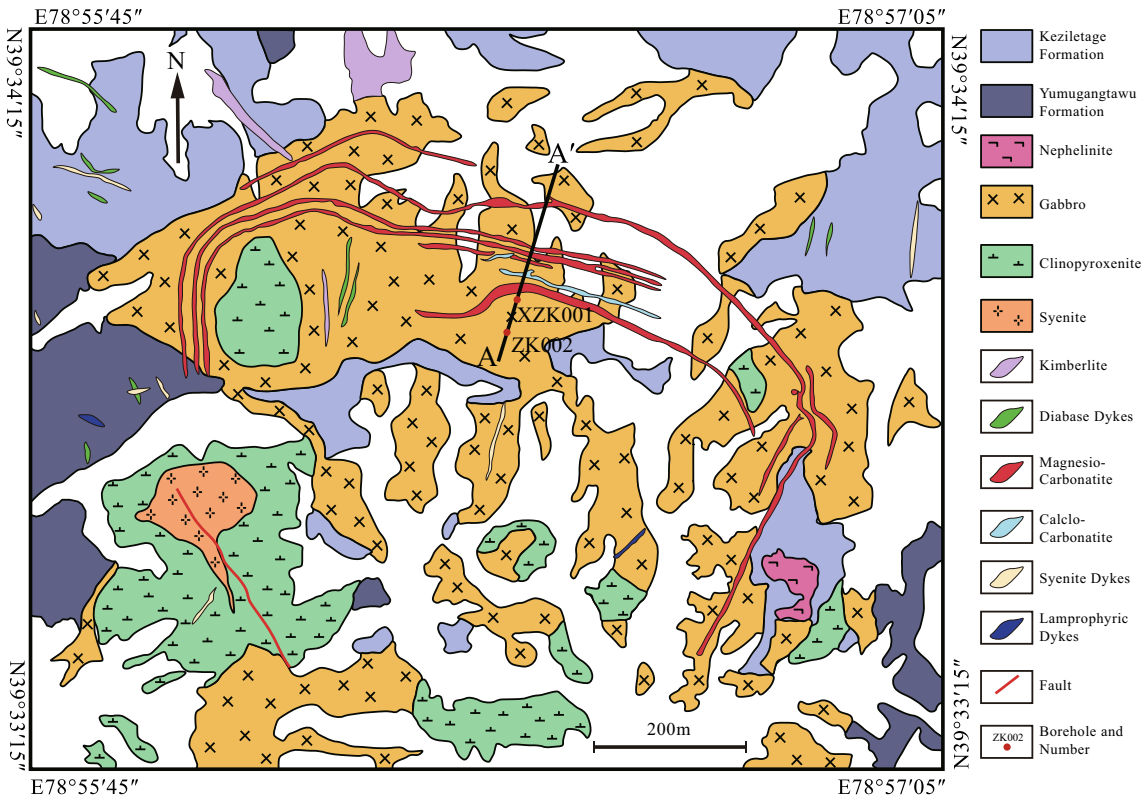

Fig. 3 Geological sketch map of the ultrabasic-alkaline complex and the location of the carbonatites in Wajilitag, Xinjiang (modified from Cheng et al. 2018)

Ore deposit types

This paper mainly discusses REE deposits in the Early Permian, so older or younger deposits (or occurrences) are not involved currently. Based on metallogenic characteristics, there are two types of rare earth mineralization related to Early Permian alkaline rocks are identified in the northern margin of the Tarim Craton as follows: (1) mineral system associated with carbonatites, typically the Wajilitag deposit and (2) mineralization in alkaline complexes, with typical as the Boziguoer and Yilanlik deposits.

Mineral system associated with carbonatites

Carbonatites are the main host of Nb–Ta, Fe-apatite, Nb-REE and fluorite mineralization, both magmatic and hydrothermal (Mariano 1989). Of these, the largest include Bayan Obo (China), Mountain Pass (USA) and Palabora (also spelled Phalaborwa, South Africa; Pirajno 2009). Carbonatite-related Fe-apatite, Nb–Ta, and Nb-REE deposits (e.g., Tomtor, Karasug, Beloziminskoe) are numerous in the Siberian Craton and surrounding orogenic belts (Seltmann et al. 2010). The Mountain Pass carbonatite typically contains bastnasite-parisite as primary magmatic minerals, albeit in a late-stage carbonatite (Castor 2008). Hydrothermal REE minerals are more common, forming polycrystalline aggregates, veinlets and interstitial fillings, and are usually associated with barite, fluorite and monazite in varying amounts, which may or may not be economically viable. Bastnasite is one of the more important REE mineral species, together with ancylite, parisite, synchysite and monazite. Most hydrothermal carbonatite-hosted REE deposits are small and uneconomic, although it is possible that a Bayan Obo style mineral system could be found in rift-related tectonic settings (Pirajno 2009). Weathering of carbonatite complexes results in dissolution of carbonate minerals, leaving behind residual and/or supergene monazite, apatite and REE minerals, such as bastnasite, parisite and florencite, ilmenite, rutile, monazite and synchysite in the carbonatites (Lottermoser 1990). Apatite is one of the principal accessory minerals in carbonatite and alkaline complexes and in some cases, apatite can exceed 50 vol.% (Mariano 1989).

The Wajilitag REE deposit is located about 42 km southeast of the town of Bachu. The geographical coordinates of the deposit are 78°52′45″E and 39°33′45″N. The Wajilitag complex is situated in the western part of the Tarim Craton (No.10 in Fig. 1b), is 5 km in length and 1.5–3 km in width, and occupying an area of ~ 12 km^2 (Fig. 3). The mafic–ultramafic complex intrudes weakly metamorphosed

upper Devonian terrestrial clastic sequences, namely; the Keziletag and Yimugangtawu Formations.

The Wajilitag mafic–ultramafic intrusion is dominantly composed of coarse-grained clinopyroxenite, fine-grained clinopyroxenite, gabbro, olivine pyroxenite, with the lithofacies showing gradational contacts, and porphyritic olivine pyroxenite that occurs as a dyke, located in the margin of the pluton, and intruding into the clinopyroxenite at a low angle.

The carbonatite dykes are distributed in the complex's northern inner contact zone, dipping at 70–80°, and forming a concentrated area of carbonatite dykes. The carbonatites have intruded the 284–281 Ma (zircon U–Pb age) layered mafic–ultramafic intrusions and are subsequently cut across by late diabase dykes (Fig. 4; Li et al. 2007; Zhang et al. 2016). Commonly, those carbonatite dikes extending nearly W-E have an enormous output scale, displaying a ring-like morphology with a single dyke length of up to 3 km and thickness of up to 20 m (Fig. 3). The intrusion age of the diabase dykes is 272 Ma (Li et al. 2007). Therefore, the age of the carbonatite dykes is between 284 and 272 Ma. The wallrocks of carbonatite dykes are mainly pyroxenite and gabbro, which are generally fenitized due to alkali

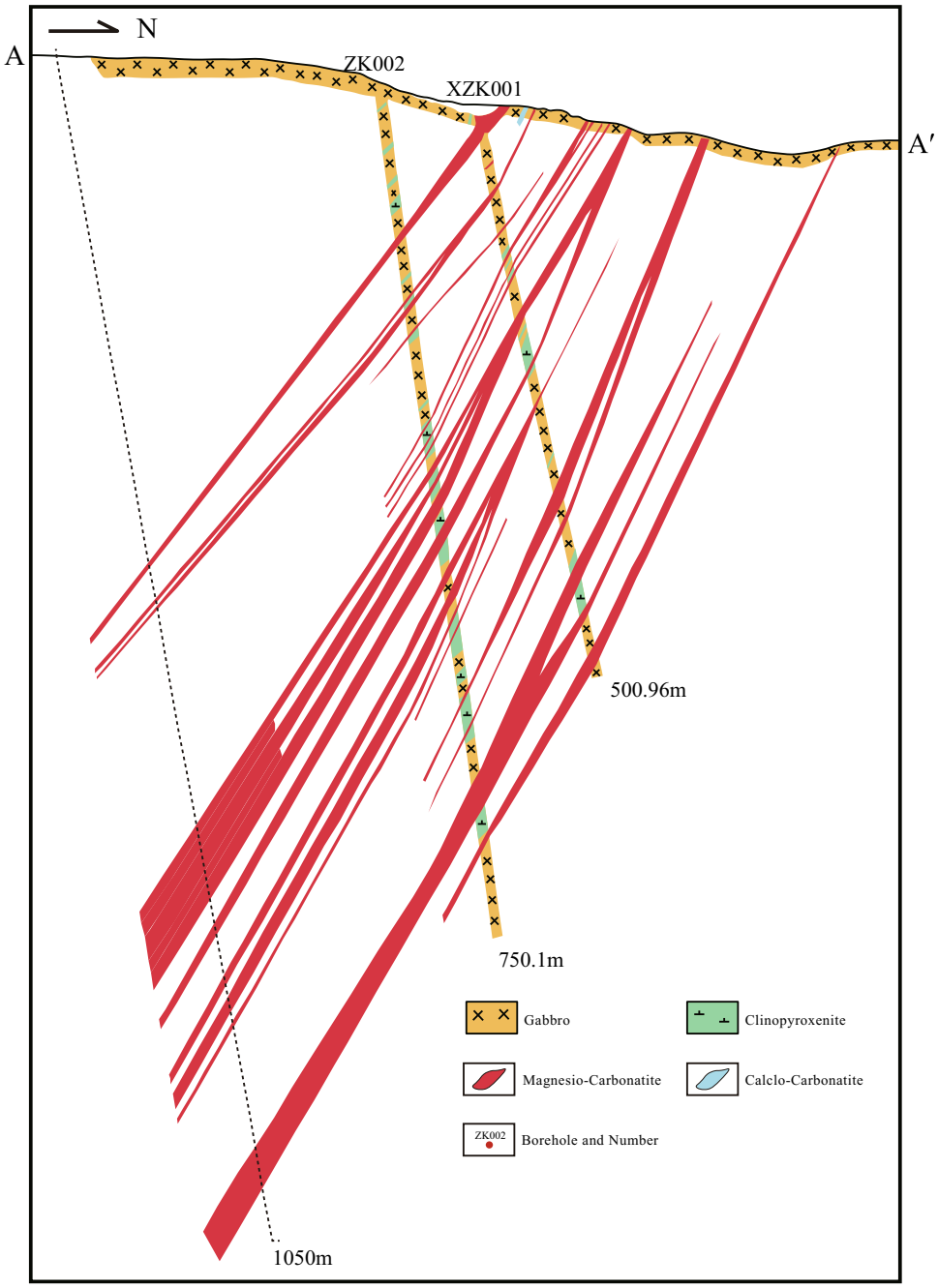

Fig. 4 The orebody section along A–A′ line of the Wajilitag REE deposit (modified from Cheng et al. 2018)

metasomatism. Recently, 24 orebodies, made up of 12 orebodies and 12 blind orebodies, have been recognized both in outcrops and drill cores, whose lengths range from 200 to 1100 m and thicknesses between 0.73 and 6.36 m, and having a measured TREO resource of 300,000 tons. The TREO grade of the carbonatite ranges from 0.51 to 1.61%, whilst the grade of associated Nb is 0.0521–0.3256% (Li and Yan 2015). The ore minerals are dominantly dolomite and calcite, and subordinate celestine, apatite, pyrite, potassium feldspar and albite. The principal rare earth minerals are monazite and fluocerite, and the main niobium-containing mineral is pyrochlorite.

Zou and Li (2006) proposed that, based on the mineral components, the primary carbonatite ores can be subdivided into three types as follows;

1. REE type: This type of ore is mainly composed of ankerite carbonatite, which is highly enriched in rare earth element content (RE_2O_3; 1.43–5.19%, average = 3.463%), low phosphorus and niobium content (P_2O_5; 0.08–1.02%, average = 0.594%; Nb_2O_5; 0.004–0.0059%).
2. REE-P type: This type of ore is composed of calcite carbonatite and calcite-dolomite carbonatite. Average ore grades are 1% RE_2O_3 (RE_2O_3; 0.32–1.55%) and 2% P_2O_5 (P_2O_5; 0.53–6.08%).
3. REE-Nb-P type: this is a REE-niobium-phosphorus enriched ore; and composed of some calcite-dolomite carbonatite. Average ore grades are 1.14% RE_2O_3 (RE_2O_3; 0.61–2.08%), 0.105% of Nb_2O_5 (Nb_2O_5; 0.021–0.299%) and 2.97% of P_2O_5 (P_2O_5; 0.70–7.38%).

Mineralization in alkaline complexes

Alkaline rocks are considered to be derived from low-degree partial melting of metasomatized mantle material, enriched in REE, HFSE and halogens (Verplanck and Van Gose 2011). However, the origin of the REE mineralization in the alkaline rocks is still the subject of debate, because the mineralization process is not well understood; even though hydrothermal processes may have played an important role (Salvi and Williams-Jones 2005). Generally, REE deposits associated with alkaline intrusions can be divided into two categories: (1) deposits in layered alkaline complexes, e.g., Nechalacho deposit (Canada), Kringlerne deposit (Greenland), Lovozero deposit (Russia); (2) deposits in dykes, veins or hydrothermal disseminations associated with alkaline intrusions, e.g., Bokan Mountain (USA), Khaldzan-Buregtey (Mongolia), Ghurayyah (Saudi Arabia). High concentrations of REE in alkaline rocks are partially due to magmatic differentiation and prolonged fractional crystallization. The REE-rich layered alkaline complexes show textures suggestive of crystal accumulation where the REE mineralization occurs in layers containing mineral cumulates that are rich in REE-bearing minerals (Dostal 2017). Cumulate textures display evidence of magmatic evolution by fractional crystallization and magma chamber processes and indicate the initial REE enrichment. The REE minerals generally accumulate in highly fractionated parts of intrusions.

The second deposit category does not show any features of crystal accumulation and associated with peralkaline rocks, which occurred as dykes, veins and disseminations (Dostal 2017). As Bokan Mountain (southeastern Alaska, USA) an example, REE mineralization forms narrow veins and linear dykes that extend out from an alkaline complex (Thompson et al. 1982). Thompson (1988) explained the observed lithologies with the fractional crystallization of evolved magma that intruded into the shallow crustal levels. Warner and Barker (1989) has identified the REE-bearing minerals in veins or dykes from the matrix of larger silicate minerals. The REE deposits related to alkaline intrusion have a variety of REE-bearing minerals, partly because magma evolution and hydrothermal processes tend to overprint primary mineralogy.

Hydrothermal alteration is widespread in alkaline complexes, mainly alkali metasomatism, but special one is known as fenitization, and the resulting rock formed is called fenites (the name comes from Fen alkaline complex in Norway; Pirajno 2013). In the late stage of magma evolution, the alkali-rich fluid was released from the magma-metasomatised wallrocks of the alkaline complex to form fenites (Le Bas 2008). The mineral composition of fenites varies greatly, depending on many factors (e.g., protolith and fluid nature). Although fenite remains mysterious, there is a strong correlation between fenitization and related mineralization, which is crucial to the formation of economic deposits (Elliott et al. 2018; Weng et al. 2021).

Although the formation process of alkaline rock-related REE deposits is not well understood, the magmatic source for the formation of economically viable deposits is derived from the metasomatised mantle. Different magmatic evolution processes have been suggested for the generation of the observed rock types at various REE-rich sites. With the differentiation and continuous evolution of magma rich in REE, P, F and other components, given the chemical properties of these components, they tend to be enriched in the final stage. The evolution of parent magma and the formation of fluid phases are crucial to forming an economic mineral deposit.

The Boziguoer deposit is located about 43 km north of Baicheng County. The geographical coordinates of the deposit are 81°55′00″E and 42°13′00″N. Tectonically, it belongs to the STOB (South Tianshan Orogenic Belt) at the northern margin of the Tarim Basin (NO.7 in Fig. 1b). The strata exposed in the mine are the upper Silurian Keketiekedaban Formation, the Lower Carboniferous Gancaohu Formation and the Lower Permian Xiaotikanlike Formation

(Fig. 5). Ore-bearing alkaline granite intrude into the Upper Silurian Keketiekedaban Formation of the thick-bedded marbles interlayered with biotite-muscovite-quartz schist (Huang et al. 2018).

A stock-like pluton intrudes into the Upper Silurian Keketiekedaban Formation marble, spreads east–west, and is composed of alkaline granite in the west and biotite granite in the east (Fig. 5). The alkaline granites can be divided into two units: (i) a porphyritic albite granite; and (ii) equigranular, medium-grained biotite-aegirine-arfvedsonite granite (Huang et al. 2014). The former is mainly distributed outside the intrusion, and occasionally distributed in the central part, whilst the latter is only exposed in the central part of the intrusion. No sharp boundary between the two units has been observed, suggesting that both units are coeval. LA-ICP-MS zircon from alkaline granites ages of ~ 288–~ 292 Ma have previously been reported by Huang et al. (2014) and Liu et al. (2014), suggesting that the Boziguoer pluton was emplaced in an extensional regime after the Carboniferous collision between the Paleozoic Tarim and SW CAOB (Central Asian Orogenic Belt), and the time is the peak of the eruption of basaltic magma in the Tarim LIP event (Huang et al. 2018; Li et al. 2017; Tian et al. 2010; Zhang et al. 2016; Shangguan et al. 2016).

The orebody's overall trend is 295°, dipping towards NNE at an angle of about 70°. The exposed area of the ore-bearing intrusion is about 1.2 km^2, with a length of about 0.8 ~ 1.1 km, and width of about 0.5 ~ 1.1 km. The deposit was discovered in 1998 and inferred to be the resource of the Boziguoer Nb–Ta-REE deposit with reserves of more than 10 Mt of Nb and 1 Mt of Ta based on average ore grades of 0.068% Nb_2O_3 and 0.0057% Ta_2O_3 (Xu et al. 2011; Huang et al. 2014). The Boziguoer deposit is mainly composed of Nb, Ta mineralization, and REE is secondary, alkaline granite has a relatively high REE content, reaching 0.058 ~ 0.1453%, with estimated REE resource is 619,500 tons (Xu et al. 2012). The ore minerals are mainly pyrochlore, followed by zircon, monazite, xenotime, bastnasite, thorite, calcium silicate, zircon, mica. Gangue minerals are mainly albite, microcline, quartz, K-feldspar, aegirine, arfvedsonite, ilmenite, and magnetite. The ores are grayish-white, and the ore minerals are mostly granular aggregates or monomers filled in between the gangue mineral particles, forming obvious sparse disseminated textures and occasionally fine vein disseminated textures (Huang et al. 2018).

Discussion

Geochronological constraints

Tarim LIP: The Tarim LIP of Permian age in northwestern China has been well surveyed and studied by geologists in the past few decades (e.g., Yang et al. 1996, 2005, 2006a, b, 2007a, 2007b; Chen et al. 1997, 1998, 2006; Jiang et al. 2004a, b, c, 2006; Li et al. 2008, 2011; Zhang et al. 2008, 2010a, b; Zhang et al. 2010c; Pirajno 2009; Zhou et al. 2009; Tian et al. 2010; Yu et al. 2011). So

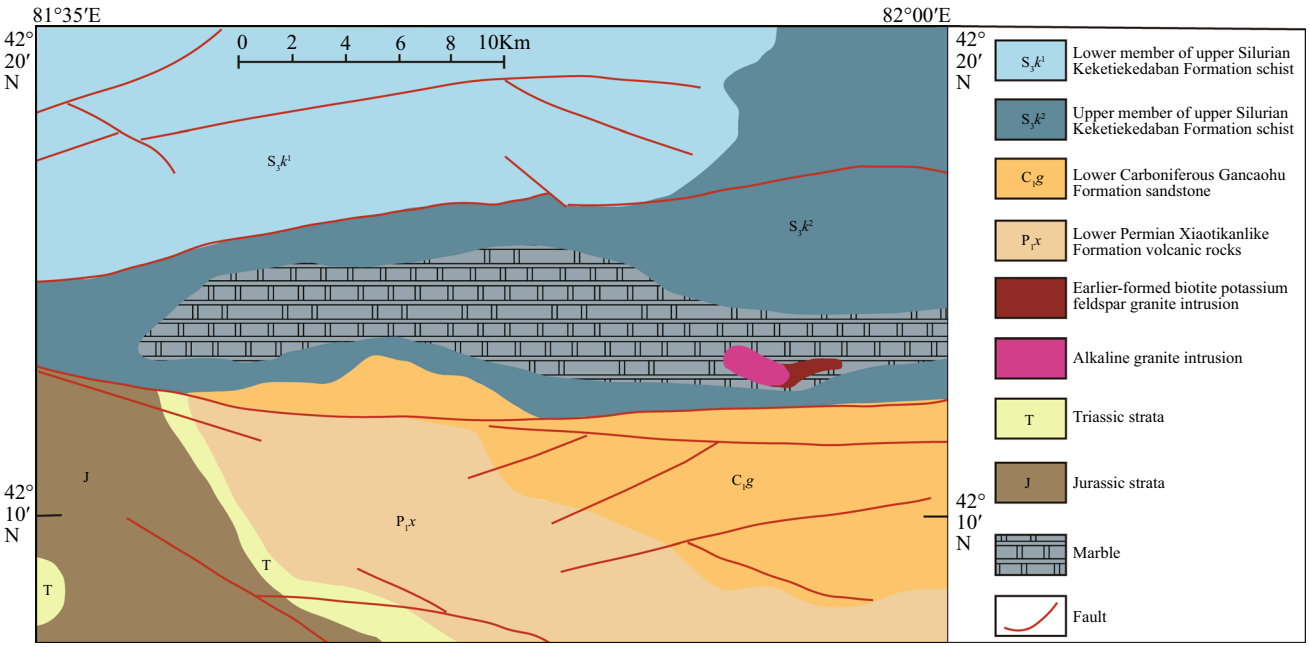

Fig. 5 Geological sketch map of the alkaline granite-type Nb–Ta–Zr-REE deposit in Boziguoer, Xinjiang (Modified from Huang et al. 2018; Liu et al. 2012)

far, published age data on the Tarim igneous rocks (e.g., basalts, mafic–ultramafic dikes, granite intrusions and volcanic rocks) show a wide range between 261 and 291 Ma, including zircon U–Pb age data by LA-ICP-MS, SHRIMP and SIMS, as well as K–Ar and ^{39}Ar–^{40}Ar (Table 2). Nevertheless, the analysis of rocks from the same locality by the same method in an individual study generated distinct results (e.g., the ages of rhyolite from Yingmai by Tian et al. 2010; Table 2), which might depend on their sampling depth/layer, because some of the rock samples come from cores collected from boreholes. The statistical results of histogram exhibit the peak age of 275–280 Ma for the igneous rock (Fig. 6), indicating that this time was the peak period of Tarim mantle plume activity. Qin et al. (2011), using a more precise Cameca IMS 1280 yielded zircon U–Pb dating on mafic–ultramafic intrusions from Beishan, obtained a relatively restricted age range between 276.8 Ma and 284.0 Ma, even though the Beishan region is far from the Tarim LIP. Moreover, these ages are consistent with the compiled zircon U–Pb age data measured by TIMS, SIMS, SHRIMP and LA-ICP-MS, illustrating a striking peak with values between 280 and 285 Ma and lie within the age range (280–300 Ma) of Pirajno et al. (2008). In addition, the ages within the Tarim basalts (Tarim LIP) age field (272–292 Ma) of Zhang et al. (2008), even though the area is located in the northwest/west of the Tarim Basin. These characteristics imply that the mafic–ultramafic intrusions in Beishan region have a geochronological genetic relationship with the Tarim flow basalts. Therefore, it can be inferred that the peak age of magma activity was ~ 280 Ma (Fig. 6), which most likely represents a period of the mantle plume activity in NW China.

Wajilitag deposit: Zhang et al. (2016) obtained SIMS U–Pb age of 281.3 ± 2.2 Ma ($n = 14$, MSWD = 1.4) and on clinopyroxenite from the Wajilitag complex, as well as three LA–ICP–MS zircon U–Pb method ages of 283.3 ± 0.88 Ma (Melagabbro), 282.4 ± 1.4 Ma (Oxide gabbro), 284.2 ± 2.8 Ma (Oxide Clinopyroxenite). Zhang et al. (2013) also dated perovskite from the Wajilitag complex by SIMS zircon U–Pb method at 299.8 ± 4.3 Ma, and also obtained 300.8 ± 4.7 and 300.5 ± 4.4 Ma for two baddeleyites samples using the same method.

Boziguoer deposit: LA-ICP-MS U–Pb zircon dating yielded ages of 275.1 ± 1.3 Ma and 275 ± 1.4 Ma for mineralized aegirine-riebeckite alkali granites in the east and west of the mine, respectively (Xu et al. 2012) and 290.1 ± 1.4 Ma for alkali granite (Huang et al. 2014). Similarly, Liu et al. (2014) performed LA-ICP-MS zircon U–Pb dating on four sample and obtained the following ages; 286.3 ± 3.5 Ma (Biotite alkali syenite), 282.2 ± 5.5 Ma (Aegirine-riebeckite alkali granite), 278.3 ± 6.5 Ma (Aegirine-riebeckite alkali granite) and 289.7 ± 4.5 Ma (Aegirine-riebeckite quartz alkali syenite).

In conclusion, the main formation time of the REE deposits related to alkaline rocks in the northern margin of Tarim Basin is almost the same as the activity time of the Tarim LIP event (Fig. 6), so it can be speculated that there is a certain genetic relationship between them.

Tectonic setting of northern margin of the Tarim Craton's REE ore deposits

Alkaline magmatism is occurred in continental anorogenic or within-plate tectonic settings and typically are related to rifts and/or extensional tectonics, mantle plume play a key role in it (Dostal 2017; Richardson and Birkett 1995; Pirajno 2021). Carbonatite is mostly produced in the background of intraplate rifts, and a relatively small amount of carbonatite terraces also occurred under the background of ocean and orogenic belts (Woolley and Kjarsgaard 2008). Therefore, in most cases, carbonatite's genesis is closely related to mantle plume activity (Hulett et al. 2016). LIPs are another important product of mantle plumes, so the mineral deposits formed during LIP formation are also potentially link of mantle plume (Pirajno 2021).

Based on previous research results, in the early Late Carboniferous (ca. 320 Ma), northward subduction of South Tianshan Ocean closed, and CAOB and Tarim Craton were collaged (Wang et al. 2018; Xiao et al. 2013). Therefore, from the late Carboniferous to Permian period, Tarim Block has entered the stage of intraplate evolution (Wang et al. 2018). Extensive post-orogenic magmatism in the entire region of the northern Tarim Craton was characterized by carbonatite and alkaline rocks and REE deposits. This locally occurring alkaline and peralkaline magmatism extends for thousands of kilometers from Xinjiang, through southern Mongolia and Inner Mongolia to North China, where granitic rocks were emplaced in two stages, first in the Permian–Triassic (300–250 Ma) and then during the Late Triassic–Cretaceous (210–120 Ma; Hong et al. 1996, 2004; Jahn 2004). Therefore, the granitic magmatism formed in Early Permian is potentially related to the Tarim LIP event, and the Tarim LIP covers large areas of northern Xinjiang with ages spanning ages from 290 to 270 Ma (Li et al. 2008, 2011; Chen et al. 2009; Zhang et al. 2013a, 2016). The intrusion of these A-Type granitic magmas occurred in the very large Permian alkaline rock belt occupying Xinjiang of magmas were probably associated with large-scale extension, accompanied by basaltic underplating, linked to the impingement of mantle plumes (Pirajno et al. 2008). In terms of results, the Tarim mantle plume affected large parts of Xinjiang and are characterized by magmatic events that include picrites and alkali basalts, tholeiitic flood basalts and carbonatite and alkaline rocks (Pirajno et al. 2008). This

Table 2 Summary of geochronological data of the Permian Tarim igneous rocks

Location	Rocks	Methods	Age (Ma)	Resources
Bachu	Syenite	Zircon SHRIMP	273.7 ± 1.5	Zhang et al. (2008)
Bachu	Quartz syenite	Zircon LA-ICP-MS	274.0 ± 2.0	Zhang et al. (2008)
Bachu	Syenite	Zircon LA-ICP-MS	281.0 ± 4.0	Li et al. (2007)
Bachu	Syenite	Zircon LA-ICP-MS	282.0 ± 3.0	Li et al. (2007)
Bachu	Syenite	Zircon LA-ICP-MS	281.7 ± 4.8	Li et al. (2007)
Bachu	Diabase	Zircon LA-ICP-MS	272.0 ± 6.0	Li et al. (2007)
Bachu	Syenite porphyry	Zircon SHRIMP	284.3 ± 2.8	Li et al. (2011)
Bachu	Syenite	40Ar/39Ar	277.7 ± 1.3	Yang et al. (1996)
Bachu	Syenite	Zircon SHRIMP	277.0 ± 4.0	Yang et al. (2006c)
Bachu	Syenite	Zircon SHRIMP	285.9 ± 2.6	Sun et al. (2008)
Bachu	Syenite	Zircon SIMS	279.7 ± 2.0	Wei and Xu (2011)
Bachu	Gabbro	Zircon SHRIMP	283.1 ± 3.2	Zhang et al. (2009a, b)
Bachu	Wehrlite	Zircon SIMS	278.9 ± 2.1	Wei et al. (2014b)
Bachu	Wehrlite	Zircon SIMS	278.4 ± 2.1	Wei et al. (2014b)
Bachu	Diorite	Zircon SHRIMP	275.2 ± 1.2	Zou et al. (2015)
Bachu	Alkali diabase	Zircon SHRIMP	281.4 ± 1.7	Zou et al. (2015)
Bachu	Quartz syenite	Zircon SHRIMP	273.0 ± 3.7	Chen et al.(2009)
Bachu	Clinopyroxenite	Zircon SIMS	283.2 ± 2.0	Shangguan et al. (2016)
Bachu	Diabase	40Ar/39Ar	285.4 ± 8.5	Zhang et al. (2010c)
Keping	Diabase	40Ar/39Ar	274.1 ± 2.4	Zhang et al. (2010c)
Keping	Basalt	40Ar/39Ar	271.9 ± 3.7	Zhang et al. (2010c)
Keping	Basalt	40Ar/39Ar	282.9 ± 1.6	Zhang et al. (2010c)
Keping	Basalt	Zircon LA-ICP-MS	275.0 ± 13.0	Li et al. (2007)
Keping	Volcanic tuff	Zircon LA-ICP-MS	291.0 ± 10.0	Li et al. (2007)
Keping	Gabbro	Zircon LA-ICP-MS	274.0 ± 15.0	Li et al. (2007)
Keping	Basalt	Zircon SHRIMP	279.0 ± 4.5	Chen et al. (2009)
Yingan	Basalt	40Ar/39Ar	287.3 ± 4.0	Wei et al. (2014a)
Yingan	Basalt	40Ar/39Ar	287.9 ± 3.1	Wei et al. (2014a)
Yingan	Basalt	K–Ar	287.2 ± 5.6	Yang et al. (2006a)
Yingan	Basalt	K–Ar	289.6 ± 5.6	Yang et al. (2006a)
Yingan	Basalt	40Ar/39Ar	281.8 ± 4.2	Yang et al. (2006a)
Yingan	Basalt	K–Ar	289.0 ± 6.1	Zhang et al. (2003)
Yingan	Basalt	K–Ar	272.9 ± 4.0	Zhang et al. (2003)
Yingan	Basalt	K–Ar	288.4 ± 4.4	Zhang et al. (2003)
Sishichang	Basalt	K–Ar	278.5 ± 1.4	Yang et al. (1996)
Sishichang	Basalt	40Ar/39Ar	278.0 ± 0.0	Jia et al. (1995)
Yingmai	Basalt	K–Ar	290.5 ± 4.2	Zhang et al. (2003)
Yingmai	Syenite	K–Ar	287.6 ± 2.8	Chen et al. (1998)
Yingmai	Rhyolite	Zircon SHRIMP	277.3 ± 2.5	Tian et al. (2010)
Yingmai	Rhyolite	Zircon LA-ICP-MS	290.9 ± 4.1	Tian et al. (2010)
Yingmai	Rhyolite	Zircon LA-ICP-MS	271.7 ± 2.2	Tian et al. (2010)
Yingmai	Rhyolite	Zircon LA-ICP-MS	282.9 ± 2.5	Tian et al. (2010)
Yingmai	Dacite	Zircon LA-ICP-MS	286.6 ± 3.3	Tian et al. (2010)
Kuche	Trachydacite	Zircon SIMS	287.2 ± 2.0	Shangguan et al. (2016)
Kuche	Rhyolite	40Ar/39Ar	278.0 ± 1.3	Chen et al. (1998)
Kuche	Granite	Rb–Sr	285.7 ± 17.0	Chen et al. (1998)
Kuche	Rhyolite	40Ar/39Ar	278.0 ± 23.0	Yang et al. (1996)
Tahe	Dacite	Zircon LA-ICP-MS	276.0 ± 3.0	Luo et al. (2006)
Tazhong	Basalt	40Ar/39Ar	268.9 ± 4.2	Zhang et al. (2010c)
Tazhong	Basalt	40Ar/39Ar	271.1 ± 3.5	Zhang et al. (2010c)
Taxinan	Basalt	K–Ar	289.6 ± 5.6	Li et al. (2008)

Table 2 (continued)

Location	Rocks	Methods	Age (Ma)	Resources
Taxinan	Basalt	40Ar/39Ar	290.1 ± 3.5	Yang et al. (2006a)
Taxinan	Basalt	K–Ar	292.4 ± 0.5	Liu and Li (1991)
Atushi	Gabbro	Zircon SHRIMP	276.0 ± 4.0	Zhang et al. (2010b)
Atushi	Granite	Zircon SHRIMP	278.0 ± 3.0	Zhang et al. (2010b)
Atushi	Granite	Zircon SHRIMP	278.0 ± 3.0	Zhang et al. (2010b)
Atushi	Alkaline granite	Zircon LA-ICP-MS	273.0 ± 1.0	Huang et al. (2012a, b)
Atushi	Alkaline granite	Zircon LA-ICP-MS	276.7 ± 0.9	Zhang and Zou (2013)
Atushi	Alkaline granite	Zircon LA-ICP-MS	272.4 ± 1.1	Zhang and Zou (2013)
Atushi	Alkaline granite	Zircon LA-ICP-MS	268.6 ± 1.5	Zhang and Zou (2013)
Atushi	Alkaline granite	Zircon LA-ICP-MS	268.8 ± 1.7	Zhang and Zou (2013)
Atushi	Alkaline granite	Zircon LA-ICP-MS	271.0 ± 2.2	Zhang and Zou (2013)
Atushi	Gabbro	Zircon LA-ICP-MS	262.3 ± 2.1	Zhang and Zou (2013)
Atushi	Lecuogabbro	Zircon LA-ICP-MS	261.7 ± 1.8	Zhang and Zou (2013)
Atushi	Gabbro	Zircon LA-ICP-MS	276.4 ± 1.1	Ma et al. (2016)
Atushi	Diabase	Zircon LA-ICP-MS	277.2 ± 0.9	Ma et al. (2016)
Atushi	Quartz syenite	Zircon LA-ICP-MS	275.5 ± 2.0	Ma et al. (2016)
Atushi	Alkaline granite	Zircon LA-ICP-MS	278.6 ± 1.9	Ma et al. (2016)
Atushi	Gabbro	Zircon LA-ICP-MS	274.0 ± 0.9	Yang et al. (2016)
Atushi	Quartz syenite	Zircon LA-ICP-MS	268.9 ± 1.0	Yang et al. (2016)
Baicheng	Alkaline granite	Zircon LA-ICP-MS	290.1 ± 1.4	Huang et al. (2014)

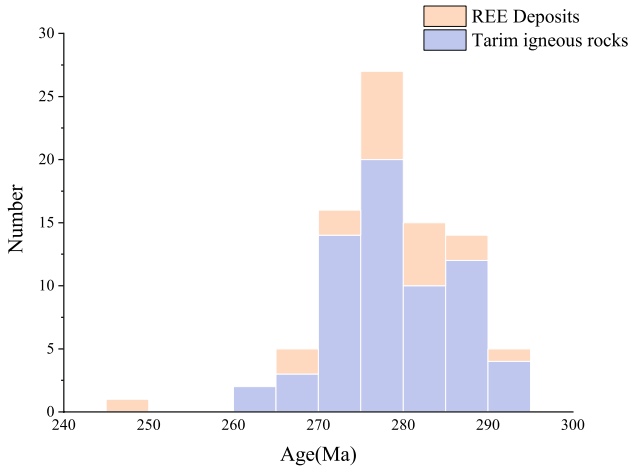

Fig. 6 Histogram of compiled age data of Early Permian igneous rocks and alkaline rock-related REE deposits in Tarim Basin (data sources see Tables 1 and 2; Zhang et al. 2016; Zhang et al. 2013; Xu et al. 2012; Liu et al. 2014)

lithological assemblage reflects the extensional tectonic setting (Dostal 2017; Woolley and Kjarsgaard 2008).

The geodynamic setting responsible for producing REE ore-forming alkaline magmatism has been variably ascribed to mantle plumes (Pirajno 2015), continental rift zones (Goodenough et al. 2016) and intracontinental fault activation due to far-field stresses (Downes et al. 2016; Slezak and Spandler 2019). In many parts of the world spatial and temporal correlations exist between carbonatites and large igneous provinces (Ernst and Bell 2010). Consequently, most of the northern margin of the Tarim Craton's REE ore deposits are interpreted to have formed in isolation of Tarim mantle plume. The carbonatite-related ore deposits (Wajilitag) were linked to the Tarim large igneous province (Pirajno and Santosh 2014), which have been suggested to have broad links to a mantle plume (Zhang et al. 2013b).

Metallogenic evolution and geodynamic processes

The large igneous province or plume of Early Permian in age occurred in the present-day southwestern part of the Tarim Craton (Yang et al. 2007a, b; Tian et al. 2010; Li et al. 2011). The exact distribution of this Early Permian LIP or plume is still debatable, with one group of scientists proposing that the plume extended in the whole Altaids or even to the Siberian Craton (Xia et al. 2004; Zhou et al. 2004; Pirajno et al. 2008), while another group suggests that the plume was only distributed in the Tarim Craton and its adjacent areas (Yang et al. 2007a, b; Tian et al. 2010; Li et al. 2011). The main evidence of the first group is from the ultramafic–mafic complexes located in the Chinese Altai, Tianshan and Beishan, which are actually either Alaskan-type complexes or results of slab-windows related to subduction of oceanic plate (Xiao et al. 2004, 2009, 2010). Also, the ages of those ultramafic–mafic complexes located in the Chinese Altai, Tianshan and Beishan are around late Carboniferous and Permian and they are subduction-related (Xiao et al. 2004, 2009, 2010; Han et al. 2010), which should not belong to any

large igneous province. Thus, the Tarim plume was probably only strictly distributed in the Tarim Craton and its adjacent areas. The mantle plume event discussed in this study is limited spatially to within southern Tianshan and Tarim, and temporally in the Early Permian (Fig. 2), which apparently differs from the plume proposed by Xia et al. (2004). Meanwhile, the Early Permian is also the most important ore-forming stage for REE deposits related to carbonatites and alkaline rocks in southern Tianshan and Tarim (Xu et al. 1998; Zou et al. 1998, 2002; Liu et al. 2004; Li and Yan 2015).

There are two stages of magmatic activity in the Tarim LIP (Xu et al. 2013, 2014): the first stage was at ~ 290 Ma, which is represented by basalt and rhyolite in the inner Tarim Basin, and the second stage occurred at ~ 280 Ma, dominated by intrusive rocks and mafic dykes in the edge of the Tarim Basin. The alkaline plutons in the northern margin of the Tarim Craton are similar to the Wajilitag carbonatites with respect to the formation age, trace elements and isotopic characteristics, and should be the product of the second stage magmatism. According to the mantle plume model of the Tarim large igneous province (Yang et al. 2007a, b), the enriched components in the Tarim lithosphere melted under the mantle plume and triggered the ~ 290 Ma magmatism. Flattening occurred when the local mantle plume ascended to the bottom of the lithosphere. Due to the thinner lithosphere at the edge of the craton, mantle plume decompression melting initiated the ~ 280 Ma magmatism (Xu et al. 2013, 2014). A large amount of mafic magma formed at ~ 280 Ma penetrated the bottom of the lower crust and underwent crystallization differentiation, resulting in the formation of a large number of intermediate-acid magma. Due to its low density, it was relatively easier for the intermediate-acid magma to rise to the shallow crustal levels to form carbonatite and alkaline rocks and associated REE deposits. Therefore, it is considered that a large amount of mafic magma at ~ 280 Ma that infiltrated into the bottom of the Tarim Craton was a necessary prerequisite for the formation of alkaline intrusions in the Tarim LIP (Cao et al. 2013).

Many REE deposits related to carbonatites and alkaline rocks in the world commonly form along the edge and interior of the ancient cratons (Huo et al. 2015a; b; Dostal 2017). For example, the Bayan Obo REE deposit is located on the northern margin of the North China Craton (Yang et al. 2019); the western margin of the Yangtze Craton has formed a world-class Dechang-Mianning REE metallogenic belt, of which the Maoniuping is the world's fifth-largest REE deposit (Liu and Hou 2017); The Mountain Pass REE deposit on the western edge of the Colorado Platform (Dostal 2017). Similarly, the REE deposits related to alkaline rocks in the Tarim Basin and its adjacent region are also located on the northern edge of the Tarim Craton, which is since these deposits were formed in the extensional setting and are closely related to the magmatic and hydrothermal system developed during the craton destruction and reworking period (Hou et al. 2015a, b; Dostal 2017). Therefore, to form economically meaningful REE deposits and refertilized thick craton margins, especially convergent margins, it is ideal for REE mineralization (Huo et al. 2015a; Liu and Hou 2017). The magma source area was previously metasomatized by subduction material to enrich REE and volatile components, or subducted sediments metasomatized subcontinental lithospheric mantle (SCLM), lithospheric destruction or asthenospheric upwelling induced metasomatic mantle or SCLM low-degree partial melting to form REE-rich carbonatite and alkaline rock parent magma made REE initially enriched (Bell and Simonetti 2010). Subsequently, after a series of magmatic evolution and hydrothermal fluid action, REE was further activated, migrated, enriched, and precipitated in tectonically weak zones to form REE deposits (Guzmics et al. 2015; Martin et al. 2013; Feng et al. 2020; Veksler et al. 2012; Hou et al. 2009; Yang et al. 2019; Klemme and Dalpe 2003; Chebotarev et al. 2019; Migdisov et al. 2016). The formation of a series of REE deposits related to alkaline rocks in the northern margin of the Tarim Basin may be due to the long-term metasomatism and reworking of the Tarim Block's lower mantle during the Meso-Neoproterozoic and Paleozoic by subduction-related sediments and recycling oceanic crust components (Zhang et al. 2008; Zhu et al. 2021). In the Early Permian, influenced by the emplacement of a mantle plume, large-scale magmatism formed the Tarim LIP, accompanied by the formation of REE-rich alkaline magma and carbonatite magma along deep faults or intraplate rifts migrated and precipitated to form ore deposits.

Conclusions

1. We have reviewed selected alkaline plutonic complex (Boziguoer) and carbonatites (Wajilitag). The carbonatites and alkaline complexes are part of the ~ 270–290 Ma Tarim LIP, which includes silica oversaturated (A-type granites) and silica-undersaturated complexes and carbonatites in the spotlight of increasing attention due to its potential to host economically viable REE resources.
2. Carbonatite and alkaline rocks-related REE deposits, which provide the majority of REE resources in the world, are the most significant global deposit types. The genesis and enrichment mechanism of REEs in such deposits are still not very clear. At present, we believe that the formation of carbonatites and alkaline rocks-related REE deposits in the northern margin of the Tarim Craton is closely related to the Tarim mantle plume.

3. The mantle plume on magmatic petrogenesis and related REE deposits occurred from ca. 290 to 270 Ma. Hence the large volume of underplating mafic magmas is the prerequisite for the formation of the coeval carbonatite intrusions and alkaline plutons of the Tarim large igneous province.

Acknowledgements We are indebted to Jingwen Mao, Bin Cui, Kezhang Qin, Lianchang Zhang, and Jianming Yang for thoughtful discussions. Many of the ideas in this paper were initiated and rectified during these discussions. Professor Li Jiliang has positively impacted the life and professional development of the authors and this article only commemorates his outstanding contribution to the cause of geology in China. This study was financially supported by funds of the National Key R&D Program of China (Grant Nos. 2018YFC0604004 and 2017YFC0601206).

References

Andersen JCØ, Rasmussen H, Nielsen TFD, Ronsbo JG (1998) The Triple Group and the Platinova gold and palladium reefs in the Skaergaard Intrusion; stratigraphic and petrographic relations. Econ Geology 93:488–509

Arndt NT, Czamanske GK, Walker RJ, Chauvel C, Fedorenko VA (2003) Geochemistry and origin of the intrusive hosts of the Noril'sk-Talnakh Cu-Ni-PGE sulfide deposits. Econ Geol 98:495–515

Begg GC, Hronsky JAM, Arndt NT, Griffin WL, O'Reilly SY, Hayward N (2010) Lithospheric, cratonic, and geodynamic setting of Ni-Cu-PGE sulfide deposits. Econ Geol 105:1057–1070

Bell K, Simonetti A (2010) Source of parental melts to carbonatites–critical isotopic constraints. Mineral Petrol 98(1–4):77–89

Cao J, Xu YG, Xing CM, Huang XL, Li HY (2013) Origin of Early Permian granitic plutons in Piqiang area, northern margin of Tarim Basin: implications for genesis of A-type granites in Tarim large igneous province. Acta Petrol Sin 29:3336–3352 ((**in Chinese with English abstract**))

Castor SB (2008) The Mountain Pass rare-earth carbonatite and associated ultrapotassic rocks, California. Canad Mineral 46:779–806

Chebotarev DA, Veksler IV, Wohlgemuth-Ueberwasser C, Doroshkevich AG, Koch-Müller M (2019) Experimental study of trace element distribution between calcite, fluorite and carbonatitic melt in the system CaCO3 + CaF2 + Na2CO3 ± Ca3(PO4)2 at 100 MPa. Contrib Mineral Petrol 174:13

Chen HL, Yang SF, Dong CW, Jia CZ, Wei G, Wang ZG (1997) Confirmation of permian basite zone in Tarim basin and its tectonic significance. Geochimica 26:77–87 (**in Chinese with English abstract**)

Chen HL, Yang SF, Jia CZ, Dong CW, Wei GQ (1998) Confirmation of Permian intermediate-acid igneous rock zone and a new understanding of tectonic evolution in the northern part of the Tarim Basin. Acta Mineral Sin 18:370–376 (**in Chinese with English abstract**)

Chen HL, Yang SF, Li ZL, Yu X, Luo JC, He GY, Lin XB, Wang QH (2009) Spatial and temporal characteristics of Permian Large Igneous Province in Tarim Basin. Xinjiang Petrol Geol 30:179–182 (**in Chinese with English abstract**)

Chen HL, Yang SF, Wang QH, Luo JC, Jia CZ, Wei GQ, Li ZL, He GY, Hu AP (2006) Sedimentary response to the Early—Mid Permian basaltic magmatism in the Tarim Plate. Geol China 33:545–552 (**in Chinese with English abstract**)

Cheng ZG, Zhang ZC, Aibai A, Kong WL, Holtz F (2018) The role of magmatic and post-magmatic hydrothermal processes on rare-earth element mineralization: a study of the Bachu carbonatites from the Tarim Large Igneous Province, NW China. Lithos 314–315:71–87

Dostal J (2017) Rare earth element deposits of alkaline igneous rocks. Resources 6:34

Downes PJ, Dunkley DJ, Fletcher IR, McNaughton NJ, Rasmussen B, Jaques AL, Verrall M, Sweetapple MT (2016) Zirconolite, zircon and monazite-(Ce) U-Th-Pb age constraints on the emplacement, deformation and alteration history of the Cummins Range Carbonatite Complex, Halls Creek Orogen, Kimberley region, Western Australia. Mineral Petrol 110:199–222

Elliott HAL, Wall F, Chakhmouradian AR, Siegfried PR, Dahlgren S, Weatherley S, Finch AA, Marks MAW, Dowman E, Deady E (2018) Fenites associated with carbonatite complexes: a review. Ore Geol Rev 93:38–59

Ernst RE, Bell K (2010) Large igneous provinces (LIPs) and carbonatites. Mineral Petrol 98:55–76. https://doi.org/10.1007/s00710-009-0074-1

Ernst RE, Buchan KL (2001) Large mafic magmatic events through time and links to mantle-plume heads. In: Ernst RE, Buchan KL (eds) Mantle plumes: their identification through time. Geol Soc Am, Special Paper 352:483–575

Feng M, Song WL, Kynicky J, Smith M, Cox C, Kotlanova M, Brtnicky M, Fu W, Wei CW (2020) Primary rare earth element enrichment in carbonatites: Evidence from melt inclusions in Ulgii Khiid carbonatite, Mongolia. Ore Geol Rev 117:103294

Goodenough KM, Schilling J, Jonsson E, Kalvig P, Charles N, Tuduri JF, Deady EA, Sadeghi M, Schiellerup H, Müller A, Bertrand G, Arvanitidis N, Eliopoulos DG, Shaw RA, Thrane K, Keulen N (2016) Europe's rare earth element resource potential: an overview of REE metallogenetic provinces and their geodynamic setting. Ore Geol Rev 72:838–856

Guo RQ, Qin Q, Zhang XF, Sun BS, Guo Y (2013) Geochronology, petrogeochemistry of Western-Kuoktagh alkaline rocks in Quruqtagh area in Xinjiang and its geological implications. J Jilin Univ (earth Science Edition) 43:457–468 (**in Chinese with English abstract**)

Guzmics T, Zajacz Z, Mitchell RH, Szabó C, Wälle M (2015) The role of liquid–liquid immiscibility and crystal fractionation in the genesis of carbonatite magmas: insights from Kerimasi melt inclusions. Contrib Mineral Petrol 169:2–18

Han CM, Xiao WJ, Zhao GC, Ao SJ, Zhang JE, Qu WJ, Du AD (2010) In-situ U-Pb, Hf and Re-Os isotopic analyses of the Xiangshan Ni-Cu-Co deposit in Eastern Tianshan (Xinjiang), Central Asia Orogenic Belt: constraints on the timing and genesis of the mineralization. Lithos 120:547–562. https://doi.org/10.1016/j.lithos.2010.09.019

Holwell DA, Keays RR (2014) The formation of Low-volume, High-tenor Magmatic PGE-Au sulfide mineralization in closed systems: evidence from precious and base metal geochemistry of the Platinova Reef, Skaergaard Intrusion, East Greenland. Econ Geol 109:387–406

Hong D, Wang SG, Han BF, Jin MY (1996) Post-orogenic alkaline granites from China and comparisons with anorogenic alkaline granites elsewhere. J Southeast Asian Earth Sci 13:13–27

Hong D, Zhang JS, Wang T, Wang SG, Xie XL (2004) Continental crust growth and the supercontinental cycle: evidence from the Central Asian orogenic Belt. J Asian Earth Sci 23:799–813

Hou ZQ, Liu Y, Tian SH, Yang ZM, Xie YL (2015a) Formation of carbonatite-related giant rare-earth-element deposits by the recycling of marine sediments. Sci Rep 5:10231

Hou ZQ, Tian SH, Xie YL, Yang ZS, Yuan ZX, Yin SP, Yi LS, Fei HC, Zou TR, Li XY (2009) The Himalayan Mianning–Dechang REE belt associated with carbonatite–alkaline

complexes, eastern Indo-Asian collision zone, SW China. Ore Geol Rev 36:65–89

Hou ZQ, Zheng YC, Geng YS (2015b) Metallic refertilization of lithosphere along cratonic edges and its control on Au, Mo and REE ore systems. Miner Depos 34:641–674 (**in Chinese with English abstract**)

Hu RZ, Tao Y, Zhong H, Huang ZL, Zhang ZW (2005) Mineralization systems of a mantle plume: a case study of the Emeishan mantle plume. Earth Sci Front 12:42–54

Huang H, Zhang ZC, Santosh M, Zhang DY (2014) Geochronology, geochemistry and metallogenic implications of the Boziguo'er rare metal-bearing peralkaline granitic intrusion in South Tianshan, NW China. Ore Geol Rev 61:157–174

Huang H, Wang T, Zhang ZC, Qie Q (2018) Highly differentiated fluorine-rich, alkaline granitic magma linked to rare metal mineralization: A case study from the Boziguo'er rare metal granitic pluton in South Tianshan Terrane, Xinjiang, NW China. Ore Geol Rev 96:146–163

Huang H, Zhang ZC, Kusky T, Santosh M, Zhang S, Zhang DY, Liu JL, Zhao ZD (2012a) Continental vertical growth in the transitional zone between South Tianshan and Tarim, western Xinjiang, NW China: Insight from the Permian Halajun A1-type granitic magmatism. Lithos 155:49–66

Huang JH, Wu CZ, Lei RX, Chen G, Xiong LM, Qin Q, Gu LX (2012b) Genesis and ore-forming model of Qieganbulak superlarge vermiculite deposit in Xinjiang. Miner Depos 31:359–368 (**in Chinese with English abstract**)

Hulett SR, Simonetti A, Rasbury ET, Hemming NG (2016) Recycling of subducted crustal components into carbonatite melts revealed by boron isotopes. Nat Geosci 9:904–908

Jahn BM (2004) The Central Asian Orogenic Belt and Growth of the Continental Crust in the Phanerozoic. In: Malpas JG, Fletcher CJ, Ali JR, Aitchison JC (eds) Aspects of the Tectonic Evolution of China. Geol Soc London, Special Publication 226:73–100

Jia CZ, Wei GQ, Yao HJ, Li LC (1995) Tectonic Evolution and regional structural geology of the Tarim Basin. In: Dong XG, Liang DG (eds) Book series on Petroleum exploration in the Tarim Basin, vol 6. Petroleum Industry Press, Beijing, pp 1–174 (**in Chinese**)

Jiang CY, Cheng SL, Ye SF, Xia MZ, Jiang HB, Dai YC (2006) Lithogeochemistry and petrogenesis of Zhongposhanbei mafic rock body, at Beishan region, Xinjiang. Acta Petrol Sin 22:115–126 (**in Chinese with English abstract**)

Jiang CY, Jia CZ, Li LC, Zhang PB, Lu DR, Bai KY (2004a) Source of the Fe riched-type high-Mg magma in Mazhartag region, Xinjiang. Acta Geol Sin 78:770–780 (**in Chinese with English abstract**)

Jiang CY, Zhang PB, Lu DR, Bai KY (2004b) Petrogenesis and magma source of the ultramafic rocks at Wajilitag region, western Tarim Plate in Xinjiang. Acta Petrol Sin 20:1433–1444 (**in Chinese with English abstract**)

Jiang CY, Zhang PB, Lu DR, Bai KY, Wang YP, Tang SH, Wang JH, Yang C (2004c) Petrology, geochemistry and petrogenesis of the Kalpin basalts and their Nd, Sr and Pb isotopic compositions. Geol Rev 50:492–500 (**in Chinese with English abstract**)

Jiang CY, Lu DR, Bai KY, Zhang PB, Ye SF, Feng JX, Chen WG (2005) Metasomatism products of continental lithosphere mantle-roseite deposits, Qieganbulake. Acta Petrol Sin 21:201–210 (**in Chinese with English abstract**)

Jin SK, Zhang ZC, Cheng ZG, Xie QH, Fei XH, Santosh M, Wang FY (2019) Compositions of olivine from the Wajilitag mafic-ultramafic intrusion of the Permian Tarim Large Igneous Province, NW China: Insights into recycled pyroxenite in a peridotite mantle source. J Asian Earth Sci 171:9–19

Jowitt SM, Williamson MC, Ernst RE (2014) Geochemistry of the 130 to 80 Ma Canadian High Arctic large igneous province (HALIP) event and implications for Ni-Cu-PGE prospectivity. Econ Geol 109:281–307

Klemme S, Dalpé C (2003) Trace-element partitioning between apatite and carbonatite melt. Am Mineral 88(4):639–646

Le Bas MJ (2008) Fenites associated with carbonatites. Canad Mineral 46:915–932

Li BQ, Meng GL, Cao X, Cao JF, Fan BC, Wang B (2015) Ore-forming geological background of the Tianshan Mountains-Pamir region in Central Asia. Geol Bull China 34:686–695 (**in Chinese with English abstract**)

Li DX, Yang SF, Chen HL, Cheng XG, LiK JXL, Li ZL, Li YQ, Zou SY (2014) Late Carboniferous crustal uplift of the Tarim plate and its constraints on the evolution of the Early Permian Tarim Large Igneous Province. Lithos 204:36–46

Li FM, Yan FL (2015) Characteristics of REE in Wajilitag carbonate type REE ore, Xinjiang. West-China Explor Engin 27:112–114 (**in Chinese with English abstract**)

Li Y, Su W, Kong P, Qian YX, Zhang KY, Zhang ML, Chen Y, Cai XY, You DH (2007) Zircon U-Pb ages of the Early Permian magmatic rocks in the Tazhong-Bachu region, Tarim Basin by LA-ICP-MS. Acta Petrol Sin 23:1097–1107 (**in Chinese with English abstract**)

Li ZL, Chen HL, Song B, Li YQ, Yang SF, Yu X (2011) Temporal evolution of the Permian Large Igneous Province in Tarim Basin in northwestern China. J Asian Earth Sci 42:917–927

Li ZL, Li YQ, Zou SY, Sun HW, Li DX (2017) The temporospatial characteristics and magma dynamics of the early Permian Tarim large igneous province. Bull Mineral Petrol Geochem 36:418–431 (**in Chinese with English abstract**)

Li ZL, Yang SF, Chen HL, Langmuir CH, Yu X, Lin XB, Li YQ (2008) Chronology and geochemistry of Taxinan basalts from the Tarim Basin: evidence for Permian plume magmatism. Acta Petrol Sin 24:959–970 (**in Chinese with English abstract**)

Liu CH, Lei M, Wu CL, Yin JW, Shao XK, Yang HT (2013) Backscattered electron detection and the charactetistics of cathodoluminescence of the minerals in A-type granitoids from Boziguoer, Baicheng County, Xinjiang. J Chinese Elec Micr Soc 32:42–46 (**in Chinese with English abstract**)

Liu CH, Wu CL, Gao YH, Lei M, Qin HP, Li MZ (2014) Zircon LA-ICP-MS U-Pb dating and Lu-Hf isotopic system of A-type granitoids in South Tianshan, Baicheng County, Xinjiang. Acta Petrol Sin 30:1595–1614 (**in Chinese with English abstract**)

Liu CH, Yin JW, Wu CL, Cai J, Shao XK, Yang HT, Gao YH, Lei M, Xu HM, Wang J (2012) Mineralogy and temperature of magma generation for A-type granitoids in Boziguoer, Baicheng County, Xinjiang. Acta Petrol Miner 31:589–602 (**in Chinese with English abstract**)

Liu CX, Xu BL, Zou TR, Lu FX, Tong Y, Cai JH (2004) Petrochemistry and tectonic significance of Hercynian alkaline rocks along the northern margin of the Tarim platform and is adjacent area. Xinjiang Geol 22:43–49 (**in Chinese with English abstract**)

Liu JQ, Li WM (1991) Petrological characteristics and ages of basalt in North Tarim. In: Jia RX (ed) Research of petroleum geology of Northern Tarim Basin in China: stratigraphy and sedimentology (I). Chinese University of Geoscience Press, Beijing, pp 194–201 (**in Chinese**)

Liu Y, Hou ZQ (2017) A synthesis of mineralization styles with an integrated genetic model of carbonatite-syenite-hosted REE deposits in the Cenozoic Mianning-Dechang REE metallogenic belt, the eastern Tibetan Plateau, southwestern China. J Asian Earth Sci 137:35–79

Long XP, Sun M, Yuan C, Kröner A, Hu AQ (2012) Zircon REE patterns and geochemical characteristics of Paleoproterozoic anatectic granite in the northern Tarim Craton, NW China: Implications for the reconstruction of the Columbia supercontinent. Precambr Res 222–223:474–487

Long XP, Yuan C, Sun M, Kröner A, Zhao GC, Wilde SA, Hu AQ (2011a) Reworking of the Tarim Craton by underplating of mantle plume-derived magmas: evidence from Neoproterozoic adakitic rocks and I-type granites in the Kuluketage area, NW China. Precambr Res 187:1–14

Long XP, Yuan C, Sun M, Xiao WJ, Zhao GC, Zhou KF, Wang YJ, Hu AQ (2011b) The discovery of the oldest rocks in the Kuluketage area and its geological implications. Sci China Earth Sci 54:342–348

Long XP, Yuan C, Sun M, Zhao GC, Wu FY, Wang YJ, Cai KD, Hu AQ (2010) Archean crustal evolution of the Tarim Craton, NW China: Zircon U-Pb and Hf isotopic constraints and implications. Precambr Res 180:272–284

Lottermoser BG (1990) Rare-earth element mineralisation within the Mt Weld carbonatite laterite, Western Australia. Lithos 24:151–167

Lu SN, Li HK, Zhang CL, Niu GH (2008) Geological and geochronological evidence for Precambrian evolution of the Tarim platform and surroungdings. Precambr Res 160:94–107

Luo JL, Zhai XX, Pu RH, He FQ, Zhao HT, Yu RL, Zhou JJ (2006) Horizon, petrology and lithofacies of the volcanic rocks in the Tahe oilfield, northern Tarim Basin. Chinese J Geol 41:378–391 (**(in Chinese with English abstract)**)

Ma Y, Zhang ZC, Huang H, Santosh M, Cheng ZG (2016) Petrogenesis of the Bashisuogong bimodal igneous complex in southwest Tianshan Mountains, China: implications for the Tarim large igneous province. Lithos 264:509–523

Mariano AN (1989) Economic geology of rare earth elements. In: Lipin BR, McKay GA (eds) Geochemistry and Mineralogy of Rare Earth Elements. Rev Mineral Geochem 21:309–337

Martin LHJ, Schmidt MW, Mattsson HB, Guenther D (2013) Element Partitioning between Immiscible Carbonatite and Silicate Melts for Dry and H2O-bearing Systems at 1–3 GPa. J Petrol 54:2301–2338

Migdisov A, Williams-Jones AE, Brugger J, Caporuscio FA (2016) Hydrothermal transport, deposition, and fractionation of the REE: Experimental data and thermodynamic calculations. Chem Geol 439:13–42

Naldrett AJ (1992) A model for the Ni-Cu-PGE ores of the Norilsk region and its application to other areas of flood-basalt. Econ Geol 87:1945–1962

Pirajno F (2009) Hydrothermal Processes and Mineral Systems. Springer, Dordrecht

Pirajno F (2013) Effects of metasomatism on mineral systems and their host rocks: alkali metasomatism, skarns, greisens, tourmalinites, rodingites, black-wall alteration and listvenites. In: Harlov D, Austrheim H (eds) Metasomatism and the chemical transformation of rock. Springer, Berlin, pp 203–252

Pirajno F (2015) Intracontinental anorogenic alkaline magmatism and carbonatites, associated mineral systems and the mantle plume connection. Gondwana Res 27:1181–1216

Pirajno F (2021) Mineral systems and their putative link with mantle plumes. Geol Soc, London, Special Publications 518: SP518-2020-2276

Pirajno F, Santosh M (2014) Rifting, intraplate magmatism, mineral systems and mantle dynamics in central-east Eurasia: an overview. Ore Geol Rev 63:265–295

Pirajno F, Mao JW, Zhang ZC, Zhang ZH, Chai FM (2008) The association of mafic-ultramafic intrusions and A-type magmatism in the Tianshan and Altay orogens, NW China: implications for geodynamic evolution and potential for the discovery of new ore deposits. J Asian Earth Sci 32:165–183

Qin KZ, Su BX, Sakyi PA, Tang DM, Li XH, Sun H, Xiao QH, Liu PP (2011) SIMS zircon U-Pb geochronology and Sr-Nd isotopes of Ni-Cu-Bearing Mafic-Ultramafic Intrusions in Eastern Tianshan and Beishan in correlation with flood basalts in Tarim Basin (NW China): Constraints on a ca. 280 Ma mantle plume. Amer J Sci 311:237–260

Richardson DG, Birkett TC (1995) Peralkaline Rock-Associated Rare Metals. In: Eckstrand OR, Sinclair WD, Thorpe RI (eds) Geology of Canadian Mineral Deposit Types. Geol Soc Am, pp 523–540

Salvi S, Williams-Jones AE (2005) Alkaline granite-syenite deposits. In: Linnen RL, Samson IM (eds) Rare-Element geochemistry and mineral deposits. Geol Assoc Canad Short Course Notes 17:315–341

Seltmann R, Soloviev S, Shatov V, Pirajno F, Naumov E, Cherkasov S (2010) Metallogeny of Siberia: tectonic, geologic and metallogenic settings of selected significant deposits. Austra J Earth Sci 57:655–706

Shangguan S, Peate IU, Tian W, Xu Y (2016) Re-evaluating the geochronology of the Permian Tarim magmatic province: implications for temporal evolution of magmatism. J Geol Soc, London 173:228–239

Shu LS, Deng XL, Zhu WB, Ma DS, Xiao WJ (2011) Precambrian tectonic evolution of the Tarim Block, NW China: new geochronological insights from the Quruqtagh domain. J Asian Earth Sci 42:774–790

Slezak P, Spandler C (2019) Carbonatites as recorders of mantle-derived magmatism and subsequent tectonic events: an example of the Gifford Creek Carbonatite Complex, Western Australia. Lithos 328:212–227

Song XY, Xiao JF, Zhu D, Zhu WG, Chen LM (2010) Advances in the study of magmatic channel system and magmatic sulfide mineralization. Earth Sci Fron 17:153–163

Song XY, Qi HW, Hu RZ, Chen LM, Yu SY, Zhang JF (2013) Formation of thick stratiform Fe-Ti oxide layers in layered intrusion and frequent replenishment of fractionated mafic magma: Evidence from the Panzhihua intrusion, SW China. Geochem Geophys 14:712–732

Sun LH, Wang YJ, Fan WM, Peng TP (2007) Petrogenesis and tectonic significance of the diabase dikes in the Bachu area, Xinjiang. Acta Petrol Sin 23:1369–1380 (**in Chinese with English abstract**)

Sun LH, Wang YJ, Fan WM, Zi JW (2008) A further discussion of the petrogenesis and tectonic implication of the Mazhashan syenites in the Bachu area. J Jilin Univ 38:8–20 (**in Chinese with English abstract**)

Thompson TB (1988) Geology and uranium-thorium mineral deposits of the Bokan Mountain granite complex, southeastern Alaska. Ore Geol Rev 3:193–210

Thompson TB, Pierson JR, Lyttle T (1982) Petrology and petrogenesis of the Bokan granite complex, southeastern Alaska. Geol Soc Am Bull 93:898–908

Tian W, Campbell IH, Allen CM, Guan P, Pan WQ, Chen MM, Yu HJ, Zhu WP (2010) The Tarim picrite-basalt-rhyolite suite, a Permian flood basalt from Northwest China with contrasting rhyolites produced by fractional crystallization and anatexis. Contrib Mineral Petrol 160:407–425

Veksler IV, Dorfman AM, Dulski P, Kamenetsky VS, Danyushevsky LV, Jeffries T, Dingwell DB (2012) Partitioning of elements between silicate melt and immiscible fluoride, chloride, carbonate, phosphate and sulfate melts, with implications to the origin of natrocarbonatite. Geochim Cosmochim Acta 79:20–40

Verplanck PL, Van Gose BS (2011) Carbonatite and alkaline intrusion-related rare earth element deposits—a deposit model. U.S. Geological Survey Open-File Report 2011–1256

Wang JT (2003) Characteristics of alkali syenite and Nb-Ta ore metallogenic in the Kuoktag, Xinjiang. West-China Explor Engin: 69–71(in Chinese)

Wang XS, Klemd R, Gao J, Jiang T, Li JL, Xue SC (2018) Final Assembly of the Southwestern Central Asian Orogenic Belt as Constrained by the Evolution of the South Tianshan Orogen:

Links with Gondwana and Pangea. J Geophys Res: Solid Earth 123:7361–7388
Warner JD, Barker JC (1989) Columbium- and rare-earth element-bearing deposits at Bokan Mountain, southeast Alaska. U.S. Bureau of Mines Open File Report 33–89
Wei X, Xu YG (2011) Petrogenesis of Xiaohaizi syenite complex from Bachu area, Tarim. Acta Petrol Sin 27:2984–3004 (**in Chinese with English abstract**)
Wei X, Xu YG (2013) Petrogenesis of the mafic dikes from Bachu and implications for the magma evolution of the Tarim Large Igneous Province, NW China. Acta Petrol Sin 29:3323–3335 (**in Chinese with English abstract**)
Wei X, Xu YG, Feng YX, Zhao JX (2014a) Plume-lithosphere interaction in the generation of the Tarim Large Igneous Province, NW China: Geochronological and geochemical constraints. Amer J Sci 314:314–356
Wei X, Xu YG, Zhang CL, Zhao JX, Feng YX (2014b) Petrology and Sr–Nd Isotopic Disequilibrium of the Xiaohaizi Intrusion, NW China: Genesis of Layered Intrusions in the Tarim Large Igneous Province. J Petrol 55:2567–2598
Weng Q, Yang WB, Niu HC, Li NB, Shan Q, Fan GQ, Jiang ZY (2021) Two discrete stages of fenitization in the Lizhuang REE deposit, SW China: Implications for REE mineralization. Ore Geol Rev 133:104090
Woolley A, Kjarsgaard B (2008) Carbonatite occurrences of the world: Map and database: Geological Survey of Canada, Open File Report 5796
Xia LQ, Xu XY, Xia ZC, Li XM, Ma ZP, Wang LS (2004) Petrogenesis of Carboniferous rift-related volcanic rocks in the Tianshan, northwestern China. Geol Soc Am Bull 116:419–433. https://doi.org/10.1130/B25243.1
Xiao WJ, Windley BF, Allen MB, Han CM (2013) Paleozoic multiple accretionary and collisional tectonics of the Chinese Tianshan orogenic collage. Gondwana Res 23:1316–1341
Xiao WJ, Zhang LC, Qin KZ, Sun S, Li JL (2004) Paleozoic accretionary and collisional tectonics of the eastern Tianshan (China): implications for the continental growth of central Asia. Amer J Sci 304:370–395. https://doi.org/10.2475/ajs.304.4.370
Xiao QH, Qin KZ, Su BX, Sun H, Tang DM, Cao MJ (2010) Studies on Xiangshan Ti-Fe and Ni-Cu sulfide ore bearing mafic-ultramafic complex from eastern Tianshan, Xinjiang. Acta Petrol Sin 26:503–522 (**in Chinese with English abstract**)
Xiao WJ, Windley BF, Yuan C, Sun M, Han CM, Lin SF, Chen HL, Yan QR, Liu DY, Qin KZ, Li JL, Sun S (2009) Paleozoic multiple subduction-accretion processes of the southern Altaids. Amer J Sci 309:221–270. https://doi.org/10.2475/03.2009.02
Xu B, Jian P, Zheng HF, Zou H, Zhang LF, Liu DY (2005) U-Pb zircon geochronology and geochemistry of Neoproterozoic volcanic rocks in the Tarim Block of Northwest China: implications for the breakup of Rodinia supercontinent and Neoproterozoic glaciations. Precambr Res 136:107–123
Xu HM, Fang JL, Wang J, Fan L (2010) Geological characteristics of Boziguoer Nb-Ta deposit in Xinjiang. Miner Depos 29:309–310 (**in Chinese**)
Xu HM, Fang JL, Zhang ZY, Wang J, Fan L, Zou TR, Liu LS, Liu J, Zhang L, Zhou YX (2011) Investigation report of niobium and tantalum deposit in Bozigoer, Baicheng county, Xinjiang Uygur Autonomous Region. Institute of Mineral Resources Chinese Academy of Geological Sciences, Beijing (**in Chinese**)
Xu HM, Zou TR, Fang JL, Xu J, Fan L, Wang J (2012) Age and genesis of Nb-Ta deposits in Boziguoer, Xinjiang. Miner Depos 31:625–626 (**in Chinese**)
Xu J, Zou TR, Yang YQ, Zhang JH, Zhou YL, Xia FR (1998) Geological tectonic environment of alkaline rock (ore) belt in the northern margin of Tarim Block, Xinjiang. Mineral Deposits 17:209–212 (**in Chinese**)
Xu J, Zou TR, Yang YQ, Zhang JH, Zhou YL, Xia FR (1999) Geological tectonic environment of alkaline rock (ore) belt in the northern margin of Tarim Block. Xinjiang Earth Sci Front 6:54 (**in Chinese**)
Xu YG, Wang Y, Wei X, He B (2013) Mantle plume-related mineralization and their principal controlling factors. Acta Petrol Sin 29:3307–3322 (**in Chinese with English abstract**)
Xu YG, Wei X, Luo ZY, Liu HQ, Cao J (2014) The early Permian Tarim large igneous province: main characteristics and a plume incubation model. Lithos 204:20–35
Yang CL, Zheng QL, Zheng Y, Guo XC (2016) The Geochemical characteristics and geological significance of Bashisuogong pluton in Soutnwest Tianshan. Xinjiang Geol 34:93–99 (**in Chinese with English abstract**)
Yang KF, Fan HR, Pirajno F, Li XC (2019) The Bayan Obo (China) giant REE accumulation conundrum elucidated by intense magmatic differentiation of carbonatite. Geology 47:1198–1202
Yang SF, Chen HL, Dong CW, Jia CZ, Wang ZG (1996) The discovery of Permian syenite inside Tarim Basin and its geodynamic significance. Geochemica 25:121–128 (**in Chinese with English abstract**)
Yang SF, Chen HL, Ji DW, Li ZL, Dong CW, Jia CZ, Wei GQ (2005) Geological process of Early to Middle Permian magmatism in Tarim Basin and its geodynamic significance. Geol J China Univ 11:504–511 (**in Chinese with English abstract**)
Yang SF, Li ZL, Chen HL, Chen W, Yu X (2006a) ^{40}Ar-^{39}Ar dating of basalts from Tarim Basin, NW China and its implication to a Permian thermal tectonic event. J Zhejiang Univ-Sci A 7:320–324
Yang SF, Li ZL, Chen HL, Dong CW, Yu X, Jia CZ, Wei GQ (2006b) Permian large volume basalts in Tarim Basin. June 2006 LIP of the Month. http://www.largeigneousprovinces.org/06jun
Yang SF, Li ZL, Chen HL, Santosh M, Dong CW, Yu X (2007a) Permian bimodal dike of Tarim Basin, NW China: Geochemical characteristics and tectonic implications. Gondwana Res 12:113–120
Yang SF, Yu X, Chen HL, Li ZL, Wang QH, Luo JC (2007b) Geochemical characteristics and petrogenesis of Permian Xiaohaizi ultrabasic dike in Bachu area, Tarim Basin. Acta Petrol Sin 23:1087–1096 (**in Chinese with English abstract**)
Yang SF, Li ZL, Chen HL, Xiao WJ, Yu X, Lin XB, Shi XG (2006c) Discovery of a Permian quartz syenitic porphyritic dike from the Tarim Basin and its tectonic implications. Acta Petrol Sin 22:1405–1412 (**in Chinese with English abstract**)
Ye HM (2014) Genesis and dynamic setting of Neoproterozoic Qieganbulake carbonatite complex from the Tarim Block. Dissertation, University of Chinese Academy of Sciences, China (in Chinese with English abstract)
Yin BX (1992) Discussion on genesis and pattern of the pelhamite deposit in Yuli, Xinjiang. Xinjiang Geol 10:6–21 (**in Chinese with English abstract**)
Yin JW, Shao XK, Yang HT, Piao TX, Xu HM (2013) Radioactive mineral characteristics of Boziguoer alkaline rocks in Baicheng, Xinjiang. Miner Depos 32:337–352 (**in Chinese**)
Yu X (2009) Magma Evolution and Deep Geological Processes of Early Permian Tarim Large Igneous Province. Dissertation, Zhejiang University (in Chinese with English abstract)
Yu X, Yang SF, Chen HL, Chen ZQ, Li ZL, Batt GE, Li YQ (2011) Permian flood basalts from the Tarim Basin, Northwest China: SHRIMP U-Pb dating and geochemical characteristics. Gondwana Res 20:485–497
Zhang HJ (2019) Geological characteristics and mineralization of the Shanghu REE deposit in Korla, Xinjiang. Dissertation, Guangzhou Institute of Geochemistry, Chinese Academy of Sciences, China (in Chinese with English abstract)
Zhang CL, Zou HB (2013) Permian A-type granites in Tarim and western part of Central Asian Orogenic Belt (CAOB):

Genetically related to a common Permian mantle plume? Lithos 172–173:47–60
Zhang SB, Ni YN, Gong FH et al (2003) A Guide to the Stratigraphic Investigation on the Periphery of the Tarim Basin. Petroleum Industry Press, Beijing (**in Chinese**)
Zhang CL, Li XH, Li ZX, Ye HM, Li CN (2008) A Permian layered intrusive complex in the Western Tarim Block, northwestern China: product of a ca. 275-Ma mantle plume? J Geol 116:269–287. https://doi.org/10.1086/587726
Zhang CL, Li ZX, Li XH, Xu YG, Zhou G, Ye HM (2010a) A Permian large igneous province in Tarim and Central Asian orogenic belt, NW China: Results of a ca. 275 Ma mantle plume? Geol Soc Am Bull 122:2020–2040
Zhang CL, Xu YG, Li ZX, Wang HY, Ye HM (2010b) Diverse Permian magmatism in the Tarim Block, NW China: genetically linked to the Permian Tarim mantle plume. Lithos 119:537–552
Zhang YT, Liu JQ, Guo ZF (2010c) Permian basaltic rocks in the Tarim Basin, NW China: implications for plume-lithosphere interaction. Gondwana Res 18:596–610. https://doi.org/10.1016/j.gr.2010.03.006
Zhang CL, Zou HB, Li HK, Wang HY (2013a) Tectonic framework and evolution of the Tarim Block in NW China: a review. Gondwana Res 23:1306–1315
Zhang DY, Zhang ZC, Santosh M, Cheng ZG, Huang H, Kang JL (2013b) Perovskite and baddeleyite from kimberlitic intrusions in the Tarim large igneous province signal the onset of an end-Carboniferous mantle plume. Earth Planet Sci Lett 361:238–248. https://doi.org/10.1016/j.epsl.2012.10.034
Zhang DY, Zhang ZC, Mao JW, Huang H, Cheng ZG (2016) Zircon U-Pb ages and Hf–O isotopic signatures of the Wajilitag and Puchang Fe–Ti oxide–bearing intrusive complexes: constraints on their source characteristics and temporal–spatial evolution of the Tarim large igneous province. Gondwana Res 37:71–85. https://doi.org/10.1016/j.gr.2016.05.011
Zhang HA, Li YJ, Wu GY, Su W, Qian YX, Meng QL, Cai XY, Han LJ, Zhao Y, Liu YL (2009a) Isotopic geochronology of Permian igneous rocks in the Tarim Basin. Chinese J Geol 44:137–158 (**in Chinese with English abstract**)
Zhang ZC, Mao JW, Saunders AD, Ai Y, Li Y, Zhao L (2009b) Petrogenetic modeling of three mafic–ultramafic layered intrusions in the Emeishan large igneous province, SW China, based on isotopic and bulk chemical constraints. Lithos 113:369–392
Zhao GC, Cawood PA (2012) Precambrian Geology of China. Precambr Res 222:13–54
Zhao GC, Wilde SA, Cawood PA, Sun M (2001) Archean blocks and their boundaries in the North China Craton: lithological, geochemical, structural and P-T path constrains and tectonic evolution. Precambr Res 107:45–73
Zhou MF, Lesher CM, Yang ZX, Li JW, Sun M (2004) Geochemistry and petrogenesis of 270 Ma Ni-Cu-(PGE) sulfide-bearing mafic intrusions in the Huangshan district, Eastern Xinjiang, Northwest China: implications for the tectonic evolution of the Central Asian orogenic belt. Chem Geol 209:233–257. https://doi.org/10.1016/j.chemgeo.2004.05.005
Zhou MF, Zhao JH, Jiang CY (2009) OIB-like, heterogeneous mantle sources of Permian basaltic magmatism in the western Tarim Basin, NW China: Implications for a possible Permian Large Igneous Province. Lithos 113:583–594
Zhu SZ, Huang XL, Yang F, He PL (2021) Petrology and geochemistry of early Permian mafic–ultramafic rocks in the Wajilitag area of the southwestern Tarim Large Igneous Province: insights into Fe-rich magma of mantle plume activity. Lithos 398–399:106355
Zou TR, Li QC (2006) Rare and rare earth metallic deposits in Xinjiang. Geological Publishing House, Beijing
Zou SY, Li ZL, Song B, Ernst RE, Li YQ, Ren ZY, Yang SF, Chen HL, Xu YG, Song XY (2015) Zircon U-Pb dating, geochemistry and Sr—Nd—Pb—Hf isotopes of the Wajilitag mafic dikes, and associated diorite and syenitic rocks:for magmatic evolution of the Tarim Large Igneous Province. Lithos 212–215:428–442
Zou TR, Xu J, Yang YQ, Zhang JH, Zhou YL, Wu CY, Yu SM, Wan DF, Lin YY, Xia FR, Cao YW, Chen WS (1998) Alkaline rocks and related mineralization in the northern margin of Tarim Basin, Xinjiang. Miner Depos 17:71–72 (**in Chinese**)
Zou TR, Xu J, Chen WS, Xia FR (2002) Rare and rare earth mineral deposits related to alkaline rocks on northern margin of Tarim Basin, Xinjiang, China. Miner Depos 21:845–848 (**in Chinese**)